Reviews in Mineralogy & Geochemistry
Vol. 86 pp. 463–488, 2021

Small Triple Oxygen Isotope Variations in Sulfate: Mechanisms and Applications

Xiaobin Cao

International Center for Isotope Effects Research
School of Earth Sciences and Engineering
Nanjing University
Nanjing 210023
PR China

xiaobincao@nju.edu.cn

Huiming Bao

International Center for Isotope Effects Research
School of Earth Sciences and Engineering
Nanjing University
Nanjing 210023
PR China
and
Department of Geology & Geophysics
Louisiana State University,
Baton Rouge, LA 70803
USA

bao@lsu.edu

INTRODUCTION

Sulfate is the most abundant electron acceptor in the ocean today. A large fraction of the buried organic matter in marine sediments is re-mineralized through microbial sulfate reduction (MSR) during which the sulfate is reduced to H_2S (Jørgensen 1982; Kasten and Jørgensen 2000). The H_2S can be re-oxidized to sulfate or buried as pyrite in sediments (Jørgensen 1977). The burial of pyrite ultimately contributes to the rising of atmosphere O_2 concentration (Berner and Canfield 1989). Sulfate, meanwhile, can be buried as gypsum and anhydrite in evaporites (Claypool et al. 1980; Crockford et al. 2019; Spencer 2000) or as barite in sedimentary rocks (Hanor 2000; Bao et al. 2008; Peng et al. 2011; Griffith and Paytan 2012; Crockford et al. 2016).

Sedimentary rocks can be uplifted and weathered with or without being subducted, melted, or metamorphosed. Thus, the initially buried sulfur minerals are transformed and eventually turned to sulfate under oxidizing atmosphere through pyrite oxidation and evaporite dissolution (Bottrell and Newton 2006). Any sulfur-bearing minerals in igneous and metamorphic rocks will also eventually be released as sulfate upon oxidative weathering and carried to the oceans.

The oxygen isotope composition of sulfate reveals the chemical pathways sulfate has experienced during its formation and consumption in sulfur cycling (Fig. 1). Secondary atmospheric sulfate can carry atmospheric O_3 and/or O_2 signature (Savarino et al. 2000; Harris et al. 2013; Bao 2015). At the surface, sulfate formed through sulfide mineral oxidation carries atmosphere O_2 and ambient water oxygen isotope signatures (Bao 2015). During MSR,

1529-6466/21/0086-0014$05.00 (print)
1943-2666/21/0086-0014$05.00 (online)
http://dx.doi.org/10.2138/rmg.2021.86.14

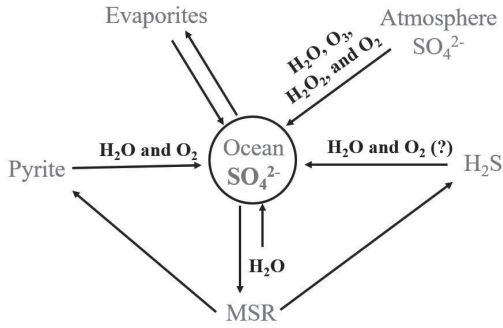

Figure 1. A global sulfur cycle in light of sulfate oxygen sources and sinks. **Grey texts** are sulfur reservoirs, **bold black texts** list the potential sources of oxygen for product sulfate during sulfur oxidation, MSR refers to microbial sulfate reduction, and arrows mark processes.

sulfate can exchange its oxygen isotope composition with ambient water via intermediates toward thermodynamic equilibrium (Wortmann et al. 2007; Zeebe 2010), erasing some or all the O_2 and water oxygen isotope signatures the sulfate may have acquired initially (Mizutani and Rafter 1973; Fritz et al. 1989; Brunner et al. 2005). Evaporite sulfate represents well the contemporary seawater sulfate of geological times (Claypool et al. 1980; Crockford et al. 2019).

Sulfate's oxygen isotope composition has received less attention than sulfate's sulfur isotope composition, due largely to oxygen's multiple sources and variable non-equilibrium isotope signatures. The normalized $^{18}O/^{16}O$ ratio or the $\delta^{18}O$ value is traditionally measured (Lloyd 1967, 1968). In the last 20 years, data on triple oxygen isotope composition (i.e., $\Delta'^{17}O \equiv \delta'^{17}O - 0.5305 \times \delta'^{18}O$) of sulfate has been accumulating. Distinctly large positive and negative ^{17}O anomalies have been found in the atmosphere and/or geological sulfate deposits (see review papers Thiemens 2006; Bao 2015; Crockford et al. 2019). These discoveries have provided exciting new insights into past atmospheric processes associated with volcanism (Bao et al. 2010), desert salt deposits (Bao et al. 2000a,b), snowball Earth (Bao et al. 2008, 2009), and gross primary productivity (Crockford et al. 2018; Hodgskiss et al. 2019).

Over the years, researchers have discovered that there are analytically resolvable differences in the $\Delta'^{17}O$ of sulfate produced by entirely mass-dependent reactions that do not involve O_3, an oxidant bearing a large ^{17}O anomaly (Bao et al. 2008; Sun et al. 2015; Killingsworth et al. 2018; Waldeck et al. 2019; Hemingway et al. 2020). We call these differences small triple oxygen isotope variations or small ^{17}O deviations (Bao 2019). Apparently intriguing patterns have been reported and geological and environmental significances inferred. However, interpreting small sulfate $\Delta'^{17}O$ data is not a trivial matter.

In this chapter, we will explore the origins of small ^{17}O deviations or small $\Delta'^{17}O$ values in sulfate. Large positive or negative sulfate ^{17}O anomalies will, therefore, not be covered here, and the readers can refer to recent reviews (Thiemens 2006; Bao 2015; Crockford et al. 2019) for details. Small sulfate $\Delta'^{17}O$ values are sensitive not only to source of oxygen but also to reaction mechanisms because equilibrium and kinetic processes generate different small non-zero $\Delta'^{17}O$ values (Young et al. 2002; Angert et al. 2004; Barkan and Luz 2007; Pack and Herwartz 2014; Bao et al. 2015). Sulfate reduction drives the remaining sulfate oxygen toward isotope equilibrium with ambient water, resulting also in a change of the small sulfate $\Delta'^{17}O$ value. Since the change during sulfate reduction process is largely controlled by ambient water isotope composition, this review will focus more on reaction mechanism and associated oxygen isotope effects on sulfate formed via pyrite oxidation. We adopt the approach of isotopologue-specific kinetic analysis (Cao and Bao 2017; Cao et al. 2019),

which helps to identify and subsequently estimate the most important parameters in determining sulfate's small $\Delta'^{17}O$ values. Isotopologue specific kinetic details during sulfate redox reactions are sketchy at this time and we will approach the problem using endmember scenarios. The intrinsic triple isotope parameters determined will then be used to construct $\Delta'^{17}O - \delta^{18}O$ space for sulfates derived from different endmember scenarios. Such $\Delta'^{17}O - \delta^{18}O$ space should be applicable not only to small $\Delta'^{17}O$ but also to the $\delta^{18}O$ or large $\Delta'^{17}O$ values, and therefore can be tested and further revised. Specific examples on riverine and lake sulfate data will be analyzed to show potential applications. Analytical methods and issues in measuring small sulfate $\Delta'^{17}O$ and future research opportunities are outlined in the end.

TRIPLE OXYGEN ISOTOPE SYSTEM

Oxygen has three stable isotopes, i.e., ^{16}O, ^{17}O, and ^{18}O. The δ notation is introduced to describe their small relative abundance variation in nature, and it is defined as (McKinney et al. 1950)

$$\delta^{17,18}O \equiv \left(\frac{^{17,18}R_{\text{sample}}}{^{17,18}R_{\text{ref}}} - 1 \right) \times 1000‰ \tag{1}$$

where $^{17,18}R$ is the mole ratio of $^{17,18}O/^{16}O$; R_{sample} and R_{ref} refer to R value for samples of interest and reference, respectively. Standard Mean Ocean Water (SMOW) (Craig 1961) (later Vienna-SMOW) is the reference material in most oxygen isotope studies. The notion of δ' is often used in triple oxygen isotope community for its many advantages (Miller 2002; Young et al. 2002). Here (Hulston and Thode 1965)

$$\delta'^{17,18}O \equiv \ln\left(\frac{^{17,18}R_{\text{sample}}}{^{17,18}R_{\text{ref}}} \right) \times 1000‰ \tag{2}$$

When oxygen isotopes fractionate in a defined process, the corresponding fractionation factor is defined as (McCrea 1950)

$$^{17,18}\alpha_{AB} \equiv \frac{^{17,18}R_A}{^{17,18}R_B} \tag{3}$$

where A and B are reactant and product or the transition state of a reaction path and the reactant, respectively. When A and B reach isotope equilibrium, α is the equilibrium isotope effect (EIE). When A and B is the transition state and the reactant, respectively, α is the kinetic isotope effect (KIE) (Bigeleisen and Wolfsberg 1958; Bao et al. 2015). EIE and KIE are two fundamental parameters of isotope fractionation. When we venture into the high-dimensional triple oxygen isotope relationship between $^{17}\alpha_{AB}$ and $^{18}\alpha_{AB}$, the community has invented a designated Greek symbol. This is the θ value or the triple isotope exponent, defined as (Mook 2000; Angert et al. 2003; Barkan and Luz 2005, 2007; Cao and Liu 2011)

$$\theta = \frac{\ln {}^{17}\alpha_{AB}}{\ln {}^{18}\alpha_{AB}} \tag{4}$$

For mass-dependent processes that have fractionation larger than a few per mil, the θ normally varies between 0.5 and 0.5305 (Bao et al. 2015; Dauphas and Schauble 2016; Hayles et al. 2017). Often, a defined process cannot be an elementary process. In that case, the θ is apparent or diagnostic for that defined process or processes. The θ value only exists when a process is specified, but any oxygen-bearing compound can have its $\delta^{17}O$ and $\delta^{18}O$ values, and thus, its small ^{17}O deviation, i.e., the $\Delta'^{17}O$ value. The $\Delta'^{17}O$ is calculated once a reference slope C is given (Angert et al. 2003; Pack and Herwartz 2014),

$$\Delta'^{17}O \equiv \delta'^{17}O - C \times \delta'^{18}O \quad (5)$$

We recommend a C value of 0.5305 mainly because this value is the triple oxygen isotope exponent at high-temperature limit for all equilibrium processes (Cao and Liu 2011; Pack and Herwartz 2014). Detailed arguments can be found in Bao et al. (2016).

SULFOXYANIONS–WATER OXYGEN ISOTOPE EXCHANGE

Sulfur has multiple sulfoxyanion species. Among them, sulfate (SO_4^{2-}) is the final stable form during the oxidation of sulfur-bearing compounds while sulfite (SO_3^{2-}) is arguably the most important intermediate with thiosulfate ($S_2O_3^{2-}$) being somewhat important during pyrite oxidation. The kinetic and equilibrium oxygen isotope exchange between the three sulfoxyanions and water are crucial to interpreting oxygen isotope compositions in sulfate. They will be briefly reviewed here.

Sulfate–water system

Sulfate is a non-labile oxyanion. Experimental results indicate its oxygen isotope composition remains unchanged for 10^9 years at most Earth surface conditions (Zak et al. 1980; Chiba and Sakai 1985; Rennie and Turchyn 2014). The preservation of large positive and negative non-mass-dependent ^{17}O anomalies from ~30 Ma (Bao et al. 2010), 635 Ma (Bao et al. 2008, 2009), and from the mid- and early Proterozoic samples (Crockford et al. 2018; Hodgskiss et al. 2019) attests to sulfate oxygen's endurance. When microbial sulfate reduction occurs, however, the sulfate in solution can exchange oxygen isotopes with water via intermediate sulfite due to reversibility of enzymatic reactions (see section *Microbial Sulfate Reduction*).

Sulfate $\delta^{18}O$ has been observed to be 14.8‰ to 28‰ higher than that of ambient water during MSR (Zeebe 2010; Brunner et al. 2012; Antler et al. 2017; Bertran et al. 2020). The variation may reflect different degrees of reversibility. At 0 °C to 150 °C, the equilibrium oxygen isotope fractionation between sulfate and water is predicted computationally to follow (Zeebe 2010)

$$1000 \times \ln {}^{18}\alpha^{EQ}_{SO_4^{2-}-H_2O} = 2.68 \times 10^6 \times T^{-2} - 7.45 \quad (6)$$

where T is the temperature in Kelvin. At 25 °C, 1000 ln $\alpha^{EQ}_{SO_4^{2-}-H_2O}$ is at ~ 23‰.

Currently, there is no experimental or theoretical calibration of the equilibrium triple oxygen isotope exponent for sulfate–water system, i.e. $\theta^{EQ}_{SO_4^{2-}-H_2O}$. In this volume, equilibrium θ values for a series of sulfate minerals and water, i.e. $\theta^{EQ}_{SM-H_2O}$, were estimated theoretically to range from 0.5242 to 0.5246 (Schauble and Young 2021, this volume). Because $\theta^{EQ}_{CO_3^{2-}-H_2O}$ is determined to be slightly smaller than $\theta^{EQ}_{calcite-H_2O}$ (Guo and Zhou 2019), $\theta^{EQ}_{SO_4^{2-}-H_2O}$ is expected to be smaller than $\theta^{EQ}_{SM-H_2O}$, and assumed to be 0.524 here. This value will be applied to construct endmember sulfates in $\Delta'^{17}O$–$\delta^{18}O$ space.

Sulfite–water system

Here we use sulfite to represent all the dissolved S(IV) species, including dissolved sulfur dioxide (SO_2(aq)), bisulfite (SHO_3^-), sulfite (SO_3^{2-}), and pyrosulfite ($S_2O_5^{2-}$) (Horner and Connick 2003). Bisulfite has two isomers, HSO_3^- where the hydrogen is bonding to sulfur and SO_3H^- where the hydrogen is bonding to oxygen. Oxygen isotope exchange between sulfite and water occurs via three proposed chemical reactions (Betts and Voss 1970; Horner and Connick 2003).

$$SO_3H^- + H^+ \underset{k_{-7a}}{\overset{k_{7a}}{\rightleftharpoons}} SO_2 + H_2O \quad (7a)$$

$$\left(SO_3H^-\right)^* + SHO_3^- \underset{k_{-7b}}{\overset{k_{7b}}{\rightleftharpoons}} \left(SO_2\right)^* + \left(H_2O\right)^* + SO_3^{2-} \quad (7b)$$

$$\left(SO_3H^-\right)^* + SHO_3^- \underset{k_{-7c}}{\overset{k_{7c}}{\rightleftharpoons}} S_2\left(O_2\right)^* O_3^{2-} + \left(H_2O\right)^* \tag{7c}$$

where '*' denotes oxygen from the SO_3H^- species prior to exchange. When bisulfite is the dominant species, the exchange rate is determined by (Horner and Connick 2003)

$$r_{ex} = \frac{1}{3}\left(k_{7a}\left[H^+\right] + k_{7bc}\left[SHO_3^-\right]\right) \tag{8}$$

where at 25 °C k_{7a} and k_{7bc} ($k_{7bc} = k_{7b} + k_{7c}$) are $1.4 \times 10^8\ M^{-1}s^{-1}$ and $8.0 \times 10^3\ M^{-1}s^{-1}$, respectively (Horner and Connick 2003). When sulfite is the dominant species, the exchange rate is (Horner and Connick 2003)

$$r_{ex} = \frac{1}{3}\left(k_{7a} + k_{7bc}\frac{\left[SO_3^{2-}\right]}{Q_2}\right)\frac{\left[H^+\right]^2}{Q_2}\frac{Q_4}{1+Q_4} \tag{9}$$

where

$$Q_2 = \frac{\left[SO_3^{2-}\right]\left[H^+\right]}{\left[SHO_3^-\right]}, \quad Q_4 = \frac{\left[SO_3H^-\right]}{\left[HSO_3^-\right]}$$

The values of Q_2 and Q_4 are $10^{-6.34}$ and 4.9, respectively (Horner and Connick 2003). Considering internal consistency, we adopt the value 4.9 instead of the newly determined result 2.7 (Eldridge et al. 2018) for Q_4 because k_{7a} and k_{7bc} were initially determined using Q_4 of 4.9. Using the values of k_{7a}, k_{7bc}, Q_2, and Q_4 given above and 0.75 for the activity coefficient of hydrogen ion $[H^+]$ at pH 8.9 and $[SO_3^{2-}]$ at 0.3 M, we estimated the half-life of sulfite–water oxygen exchange to be 75 s, which is consistent with the experimentally obtained 78 s at the given chemical condition (Betts and Voss 1970). At pH 9.8, the exchange half-life is estimated to be 79 min, being consistent with the 82 min determined by Betts and Voss (1970) but is inconsistent with the 24.3 min determined by Wankel et al. (2014). The cause for the discrepancy is unclear but may have to do with the pH buffer glycine used by Wankel et al. (2014) because glycine, a potentially general acid catalyst (Horner and Connick 2003), could have catalyzed the exchange reactions. At pH of 7, the half-life is estimated to be less than 1s for dilute solutions (e.g. 0.1 mM). In addition, exchange rate is dependent on $[SO_3^{2-}]$, as shown in Equations (8) and (9). These analyses demonstrate that oxygen isotope exchange between sulfite and water is rapid, especially at low pH conditions.

Although the equilibrium isotope fractionation between individual sulfite species and water varies only with temperature, the fractionation between total dissolved S(IV) and water, i.e. $^{18}\alpha^{EQ}_{SO_3^{2-}-H_2O}$, is pH dependent because sulfite species partition is pH dependent (Müller et al. 2013b). The value of $1000\ln{}^{18}\alpha^{EQ}_{SO_3^{2-}-H_2O}$ at 23 °C was determined to be 11.5‰ and 7.9‰ at pH 7.2 and 8, respectively (Brunner et al. 2006). The pH and temperature dependence of $1000\ln{}^{18}\alpha^{EQ}_{SO_3^{2-}-H_2O}$ was also observed subsequently and determined to be (Wankel et al. 2014),

$$1000 \times \ln{}^{18}\alpha^{EQ}_{SO_3^{2-}-H_2O} = 1000 \times \ln\left(\frac{13.61 - 0.299 \times pH - 0.081 \times t}{1000} + 1\right) \tag{10}$$

where t is temperature in Celsius in the range of 2 °C to 95 °C and pH in the range of 4.5 to 9.8. According to Equation (10), the $1000\ln{}^{18}\alpha^{EQ}_{SO_3^{2-}-H_2O}$ at 23 °C should be 9.5‰ and 9.3‰ at pH 7.2 and 8, respectively. This is different from an experimentally determined $1000\ln{}^{18}\alpha^{EQ}_{SO_3^{2-}-H_2O}$ value of 15.2‰ at 22 °C, a value displaying no pH dependence in the range of 6.3 to 9.7 (Müller et al. 2013b). The difference between the three experimental studies is

as large as 7.3‰. As of now, the value of $1000\ln{}^{18}\alpha^{EQ}_{SO_3^{2-}-H_2O}$ lies between 7.9‰ and 15.2‰ at 22 °C and further calibration effort is warranted. This issue will be revisited later.

Triple oxygen isotope exponent for equilibrium sulfite–water exchange, i.e., $\theta^{EQ}_{SO_3^{2-}-H_2O}$, has not been calibrated. However, due to the overall S–O bonding similarity between SO_4^{2-} and SO_3^{2-}, we assume that $\theta^{EQ}_{SO_3^{2-}-H_2O} \approx \theta^{EQ}_{SO_4^{2-}-H_2O}$ and thus the value 0.524 is adopted for $\theta^{EQ}_{SO_3^{2-}-H_2O}$ to construct endmember sulfates in $\Delta'^{17}O$–$\delta^{18}O$ space.

Thiosulfate–water system

Although thiosulfate (SSO_3^{2-}) has a chemical structure similar to that of sulfate, experimental results show that thiosulfate readily exchange oxygen isotopes with water (Pryor and Tonellat 1967; Betts and Libich 1971). At pH > 5, oxygen exchange between thiosulfate and water proceeds mainly through thiosulfate–sulfite–water exchange pathway in which sulfite acts as a catalyst (Betts and Libich 1971). Two chemical reactions are responsible for the oxygen exchange (Betts and Libich 1971)

$$SO_3^{2-} + S^*SO_3^{2-} \underset{k_{-11a}}{\overset{k_{11a}}{\rightleftharpoons}} SSO_3^{2-} + {}^*SO_3^{2-} \tag{11a}$$

$$SO_3^{2-} + H_2{}^*O \underset{k_{-11b}}{\overset{k_{11b}}{\rightleftharpoons}} S^*O_3^{2-} + H_2O \tag{11b}$$

where '*' denotes the sulfur and oxygen prior to the change in thiosulfate and water, respectively. Reaction (11b) refers to an overall oxygen exchange reaction represented by chemical reactions (7a–7c). When pH is in the range of 5 to 10, the oxygen exchange rate between thiosulfate and sulfite is far slower than the one between sulfite and water, hence the overall exchange rate between thiosulfate and water can be approximated by the slower step, i.e., the exchange rate between thiosulfate and sulfite (Betts and Libich 1971)

$$r_{ex} = 3k_{11a}\left[SSO_3^{2-}\right]\left[SO_3^{2-}\right] \tag{12}$$

and at 25 °C $k_{11a} = 2.07 \times 10^{-4}\ M^{-1}s^{-1}$. When pH goes up to the range of 10 to 11, the two rates are comparable, therefore, the overall oxygen exchange rate is determined by both thiosulfate–sulfite and sulfite–water exchange rates. At even higher pH, e.g., above 11, the rate of thiosulfate–sulfite exchange is faster than that of sulfite–water exchange, thus, the overall exchange rate can be estimated by Equation (9). In acidic condition (pH < 4), thiosulfate is unstable (Xu and Schoonen 1995).

No experimental or theoretical thiosulfate–water equilibrium α value is available in literature at this time. According to Betts and Libich's (1971) experiments, thiosulfate may be enriched in heavy oxygen isotopes relative to sulfite, and the ^{18}O enrichment is about 1‰ at pH of 10.8 and *t* of 50.3 °C. At lower temperature, the enrichment is expected to be larger. Similarly, no θ calibration has been conducted for thiosulfate–water equilibrium. For now, we will adopt the value 0.524 to construct endmember sulfates in $\Delta'^{17}O$–$\delta^{18}O$ space.

MICROBIAL SULFATE REDUCTION (MSR)

Early on, researchers found that sulfate exchanges its oxygen isotopes with water through intermediates during the reversible microbial sulfate reduction (MSR) processes (Mizutani and Rafter 1973; Fritz et al. 1989) (Fig. 2). Several models have been proposed to calculate sulfate $\delta^{18}O_{SO_4}$ during MSR (Brunner et al. 2005, 2012; Turchyn et al. 2010; Antler et al. 2013, 2017; Wankel et al. 2014; Bertran et al. 2020). Generally, the $\delta^{18}O_{SO_4}$ is a function of the initial $\delta^{18}O_{SO_4}$, $\delta^{18}O_{SO_3}$, $\delta^{18}O_{AMP}$ (AMP: adenosine monophosphate), $\delta^{18}O_{H_2O}$, the rate and the

reversibility of the involved individual steps between sulfate and sulfite (Brunner et al. 2012; Bertran et al. 2020) (Fig. 2). In the meantime, the $\delta^{18}O_{SO3}$ and $\delta^{18}O_{AMP}$ themselves vary with oxygen exchange rates between sulfite, AMP, and water, as well as their respective oxidation rates to APS (Adenosine−5′-phosphosulfate). All these parameters are case specific and have so far been under-constrained. Therefore, we are not attempting to explore all the possibilities here. Instead, only the endmember case when the MSR processes approaching thermodynamic equilibrium caused by the high level of MSR reversibility (Zeebe 2010) is considered. For this case, sulfate oxygen isotope composition is calculated by,

$$^{17,18}R_{SO_4^{2-}} = {}^{17,18}\alpha^{EQ}_{SO_4^{2-}-H_2O}\,{}^{17,18}R_{H_2O} \quad (13)$$

and $^{17,18}\alpha_{SO4\text{-}H2O}{}^{EQ}$ estimated by Equation (6), and the θ value is at 0.524.

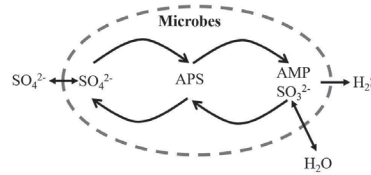

Figure 2. Sketch of a model for microbial sulfate reduction. The grey dashed circle marks the cell membrane; oxygen exchange between sulfate and water is achieved by sulfite and AMP exchange with ambient water and oxidized back to sulfate internally; APS and AMP are adenosine-5′-phosphosulfate and adenosine monophosphate, respectively.

SULFIDE OXIDATION MECHANISMS

The oxidation of mineral sulfides to sulfate on the Earth surface occurs mostly in aqueous conditions. The process involves multiple reaction steps and multiple sulfur intermediates. Oxygen from dissolved O_2 and water can both be incorporated into sulfate. Atmospheric O_2 (23.88‰ in $\delta^{18}O$ and −0.553‰ in $\Delta'^{17}O$ according to Barkan and Luz 2011) and water have very different $\delta^{18}O$ and $\Delta'^{17}O$. In addition to this source difference, the relative proportion of these two sources depends on the oxidation pathway, which differs in equilibrium and kinetic isotope effects. All these factors should be considered in interpreting sulfate $\delta^{18}O$ value as summarized in van Stempvoort and Krouse (1993) and must be considered in interpreting sulfate's small $\Delta'^{17}O$ as well. There are uncalibrated parameters for $\delta^{18}O$ and even more uncalibrated ones for triple oxygen isotope behaviors during sulfide oxidation processes. In this section, we begin to unravel factors that matter to sulfate triple oxygen isotope compositions by examining endmember cases.

Thiosulfate oxidation on pyrite surface

Pyrite oxidation has been extensively studied due to its detrimental environmental impact and connection to the mineral resource. Electrochemical oxidation is the widely accepted mechanism (Luther 1987; Moses et al. 1987; Moses and Herman 1991; Rimstidt and Vaughan 2003). Previous studies show that factors, such as Eh, pH, oxidant type and concentration, grain size, can affect the oxidation process. Readers should refer to (Rosso and Vaughan 2006; Chandra and Gerson 2010) for comprehensive reviews on these topics. Here we focus on the oxygen isotope compositions in sulfate formed via pyrite oxidation in responding to these factors.

Pyrite is a semiconductor, and its oxidation and reduction happen at different sites on the pyrite surface. According to the proposed electrochemical model (Rimstidt and Vaughan 2003), three distinct reaction steps are involved. First, O_2 or Fe^{3+} acquires electrons from an Fe^{2+} site, i.e., the cathodic site, and Fe^{2+} is oxidized to Fe^{3+}. Second, electrons are transferred from the sulfur site, i.e., the anodic site, to the Fe^{3+} at the cathodic site. The third step is

water molecule reacting with sulfur to form sulfoxyanion at the anodic site. These reactions are repeated until thiosulfate is formed. At low pH conditions, thiosulfate is further oxidized to sulfate on the surface (Rimstidt and Vaughan 2003). All the oxidation steps on the sulfur (anodic) sites involve only water, no O_2 bonds directly with S. We can, therefore, conclude that oxygens in sulfate formed by thiosulfate oxidation on pyrite surface at low pH conditions all come from water. Sulfate of this origin serves as an endmember case. Further elaboration of this endmember is given below.

(1) Pyrite oxidation via Fe^{3+} happens via thiosulfate at surface (not in solution) at low pH. Observed apparent sulfate–water oxygen isotope fractionation, $\Delta\delta^{18}O_{SO_4-H_2O}$, during pyrite oxidation by Fe^{3+} is in the range of 2.3‰ to 2.9‰ (Balci et al. 2007; Mazumdar et al. 2008; Heidel and Tichomirowa 2011). However, observed apparent $\Delta\delta^{18}O_{SO_4-H_2O}$ during sulfite oxidation by Fe^{3+} in solution is ~ 5.9‰ (Müller et al. 2013a) or 8.2‰ (Balci et al. 2012 and section *Sulfite oxidation by Fe^{3+} in solution*). A likely cause of this discrepancy is that thiosulfate on pyrite surface does not enter solution but is oxidized by Fe^{3+} on pyrite surface straight to sulfate at acidic conditions. This conclusion is also supported by the experiment that showed sulfate was the first dominant sulfur species detected in solution (Borilova et al. 2018). Indeed, thiosulfate is unstable in solution and will be converted to sulfite at this low pH conditions (see the next section for details).

One may argue that this discrepancy is caused by sulfite being out of oxygen isotope equilibrium with water when sulfite is oxidized to sulfate by Fe^{3+} in solution. Müller et al. (2013a) do conclude that sulfite–water was not at oxygen isotope equilibrium for their sulfite oxidation by Fe^{3+} experiments. However, if this were the case, the rate of sulfite to sulfate oxidation by Fe^{3+} would have to be faster than the rate of sulfite–water oxygen isotope exchange, which is certainly not the case. The oxidation rate is ~ $3.2\times10^{-2}\,M^{-1}s^{-1}$ for their experiments at pH 1.0 (Müller et al. 2013a). The sulfite–water exchange rate is, however, ~$1.4\times10^{8}\,M^{-1}s^{-1}$, i.e., k_{7a} for reaction (7a), at pH 1, which is ten orders of magnitude faster than the oxidation rate. Therefore, the observed small apparent disequilibrium in Muller et al.'s experiment might be caused by other factors. We suspect that the high concentrations of sulfite and Fe^{3+} used in the experiment may have slowed down sulfite–water isotope exchange due to the formation of $FeSO_3^{+}$ and $Fe_2(OH)SO_3^{3+}$ complexes in solution (Lente and Fábián 2002). At low sulfite and Fe^{3+} concentrations as in most natural solutions, however, such complexes are minimal. At low pH conditions, sulfite is in oxygen isotope equilibrium with water at all time during Fe^{3+}oxidation in the solution, especially at low sulfite and Fe^{3+} concentrations.

(2) Kinetic isotope effects are responsible for the apparently smaller $\Delta\delta^{18}O_{SO_4-H_2O}$ during pyrite oxidation by Fe^{3+}. If indeed sulfate–water oxygen isotope fractionation is smaller when going through thiosulfate oxidation on pyrite surface than going through sulfite oxidation in solution, the underlying mechanism must be explored. At this time, no study has been done on the subject. We can speculate that thiosulfate oxidation on the surface would have to break the S–S bond in addition to the formation of S–O bond, and this additional bond-breaking process adds a corresponding kinetic oxygen isotope effect to SO_3^{2-} in SSO_3^{2-} on the surface, which reduces the level of ^{18}O enrichment in final product sulfate.

(3) Thiosulfate on pyrite surface is likely at oxygen isotope equilibrium with water before being oxidized to sulfate. At low pH, the rate of oxygen isotope exchange between thiosulfate and water is high (Pryor and Tonellat 1967; Betts and Libich 1971), but the rate of thiosulfate oxidation to sulfate on pyrite surface is absent, which renders a direct rate comparison unattainable for now. However, two indirect lines of evidence suggest that the exchange rate is much higher. First, different research groups have obtained similar apparent $\Delta\delta^{18}O_{SO_4-H_2O}$ value for this oxidation process, ranging from 2.3‰ to 2.9‰, at variable overall oxidation rates (Balci et al. 2007; Mazumdar et al. 2008; Heidel and Tichomirowa 2011). If isotope exchange between sulfoxyanions and water were relatively slow, the sulfoxyanions-water system would be out of equilibrium at different degrees, and the $\Delta\delta^{18}O_{SO_4-H_2O}$ would be highly variable. Second,

the $\delta^{18}O$ of product sulfate via thiosulfate oxidation on the pyrite surface can be calculated by

$$^{18}R^{py}_{SO_4^{2-}} = \left(\frac{3}{4}\,^{18}KIE_{SSO_3^{2-}\rightarrow SO_4^{2-}}\,^{18}\alpha_{SSO_3^{2-}-H_2O} + \frac{1}{4}\,^{18}KIE_{H_2O\rightarrow SO_4^{2-}}\right)^{18}R_{H_2O} \quad (14a)$$

whereas the $\delta^{18}O$ of product sulfate via sulfite oxidation by Fe^{3+} in the solution is given by

$$^{18}R^{aq}_{SO_4^{2-}} = \left(\frac{3}{4}\,^{18}KIE_{SO_3^{2-}/Fe^{3+}\rightarrow SO_4^{2-}}\,^{18}\alpha^{EQ}_{SO_3^{2-}-H_2O} + \frac{1}{4}\,^{18}KIE_{H_2O\rightarrow SO_4^{2-}}\right)^{18}R_{H_2O} \quad (14b)$$

If $^{18}KIE_{H_2O\rightarrow SO_4}$ is assumed to be the same for these two alternative processes, the value of $^{18}KIE_{SSO_3\rightarrow SO_4} \times {}^{18}\alpha^{EQ}_{SSO_3^{2-}-H_2O}$ is roughly estimated to be ~0.994 times of that of $^{18}KIE_{SO_3/Fe^{3+}\rightarrow SO_4} \times {}^{18}\alpha^{EQ}_{SO_3^{2-}-H_2O}$ in order to fit the observations. Since $^{18}KIE_{SSO_3\rightarrow SO_4}$ is smaller than $^{18}KIE_{SO_3/Fe^{3+}\rightarrow SO_4}$ (see analysis in this subsection (2) above) and $^{18}\alpha^{EQ}_{SSO_3^{2-}-H_2O}$ and $^{18}\alpha^{EQ}_{SO_3^{2-}-H_2O}$ can be treated as the same in value (see section *Thiosulfate–water system*), the simplest explanation is that the two α^{EQ}s in Equations (14a, 14b) are both fully expressed, i.e., rapid exchange equilibrium with water, and $^{18}KIE_{SSO_3\rightarrow SO_4}$ is 0.994 times of the $^{18}KIE_{SO_3/Fe^{3+}\rightarrow SO_4}$ in this case.

Therefore, the $\delta^{18}O$ for sulfate derived from thiosulfate oxidation by Fe^{3+} on pyrite surface is determined by

$$^{17,18}R^{surf}_{SO_4^{2-}} = \left(\frac{3}{4}\,^{17,18}KIE_{SSO_3^{2-}\rightarrow SO_4^{2-}}\,^{17,18}\alpha^{EQ}_{SSO_3^{2-}-H_2O} + \frac{1}{4}\,^{17,18}KIE_{H_2O\rightarrow SO_4^{2-}}\right)^{17,18}R_{H_2O} \quad (15)$$

The related kinetic and equilibrium triple isotope effects will be constrained by Monte Carlo technique later.

Sulfite oxidation by O_2 in solution

The electrochemical model of pyrite oxidation (Rimstidt and Vaughan 2003) precludes any O_2 being incorporated into sulfate if all the oxidation steps occur on the pyrite surface. However, experimental results (Balci et al. 2007; Heidel et al. 2009; Tichomirowa and Junghans 2009; Heidel and Tichomirowa 2010; Kohl and Bao 2011) and field observations (Bao et al. 2008; Crockford et al. 2018; Killingsworth et al. 2018; Hodgskiss et al. 2019) demonstrate to variable degrees that O_2 isotope signal is incorporated in sulfate during pyrite oxidation in aerated solution, which means that thiosulfate can be released from pyrite surface to solution, even at low pH conditions. Thus, sulfite oxidation by O_2 at low pH can serve as another endmember case of sulfate formation. We elaborate on our argument below.

(1) Sulfite is an important intermediate for sulfur oxidation to sulfate. Thiosulfate decomposes to S^0 and sulfite at low pH conditions or tetrathionate ($S_4O_6^{2-}$) in the presence of pyrite (Xu and Schoonen 1995). At pH 6, tetrathionate is observed to be the most abundant intermediate (Goldhaber 1983). When oxidized to sulfate, tetrathionate is converted to sulfite first (Druschel et al. 2003). Sulfur chain shortening is suggested to be one possible mechanism (Druschel et al. 2003), although how exactly the conversion takes place is not clear (Moses et al. 1987). Regardless of the pathway thiosulfate decomposes, sulfite is the inevitable intermediate to the final oxidation product sulfate.

(2) Fe^{3+} loses out to O_2 as a competitive oxidant at low pH. While sulfite oxidation has a higher rate via Fe^{3+} than via O_2 at low pH conditions, e.g., about two orders of magnitude faster at pH 1 (Müller et al. 2013a), the Fe^{3+} oxidation pathway cannot be sustained if its reduction product Fe^{2+} is not oxidized to Fe^{3+} by O_2 quickly. At low pH conditions, the rate of Fe^{2+} oxidation by O_2 is sufficiently slow, e.g., 10^{-7} min^{-1} at pH 2 and pO_2 of 0.2 Atm (Singer and Stumm 1970), so that sulfite oxidation by O_2 should dominate the oxidation process, especially for experiments with no Fe^{3+} added initially.

(3) Sulfite maintains its oxygen isotope equilibrium with water during its oxidation by O_2 at low pH. This is logical because, as shown in the above subsection (1), sulfite–water oxygen isotope exchange rate is several orders of magnitude higher than the oxidation rate by Fe^{3+}, and the oxidation rate by $Fe^{3+}$is higher than by O_2.

(4) The final product sulfate has 1/4 of its oxygen coming from O_2 and 3/4 from water. It has been proposed that sulfite oxidation by O_2 is a radical chain reaction as described below (Zhang and Millero 1991; Kuo et al. 2006)

Initiation $$M^{n+} + SO_3^{2-} \rightarrow M^{(n-1)+} + SO_3^{\bullet -}$$

Propagation $$SO_3^{\bullet -} + \mathbf{O_2} \rightarrow SO_3\mathbf{OO}^{\bullet -}$$

$$SO_3\mathbf{OO}^{\bullet -} + SO_3^{2-} \rightarrow SO_3\mathbf{OO}^{2-} + SO_3^{\bullet -}$$

Oxidation $$SO_3\mathbf{OO}^{2-} + SO_3^{2-} \rightarrow 2SO_3\mathbf{O}^{2-}$$

Termination $$SO_3\mathbf{OO}^{\bullet -} + SO_3^{\bullet -} \rightarrow S_2O_6^{2-} + \mathbf{O_2}$$

$$SO_3\mathbf{OO}^{\bullet -} + SO_3\mathbf{OO}^{\bullet -} \rightarrow S_2O_6^{2-} + 2\mathbf{O_2}$$

in which oxygen sourced from O_2 is in bold. Because sulfite–water oxygen isotope exchange is rapid at low pH conditions, sulfite always carries equilibrated water oxygen isotope composition before being oxidized to sulfate. In the oxidation step, the product sulfate obtains its 1/4 oxygen from O_2. This mechanism is supported by sulfite (Holt et al. 1981; Müller et al. 2013a) and pyrite oxidation experiments (Tichomirowa and Junghans 2009; Kohl and Bao 2011). O_2 does not exchange oxygen isotopes with sulfite or water in the processes (Krouse et al. 1991).

Therefore, for this endmember case, i.e., sulfite oxidation by O_2 in low pH solutions, the sulfate oxygen isotope composition is determined by,

$$^{17,18}R_{SO_4^{2-}}^{D.O.} = \frac{3}{4}\,^{17,18}KIE_{SO_3^{2-}/O_2 \rightarrow SO_4^{2-}}\,^{17,18}\alpha_{SO_3^{2-}-H_2O}^{EQ}\,^{17,18}R_{H_2O} + \frac{1}{4}\,^{17,18}KIE_{O_2 \rightarrow SO_4^{2-}}\,^{17,18}R_{O_2} \quad (16)$$

The related kinetic and equilibrium triple isotope effects will be constrained by Monte Carlo technique later.

Sulfite oxidation by Fe^{3+} in solution

As discussed in the above section, thiosulfate can be released into solution and converted to sulfite before being oxidized to sulfate at low pH conditions. If this sulfite is oxidized by Fe^{3+} rather than O_2 in solution, the product sulfate will have all of its oxygens sourced from water. Here, we place sulfite oxidation by Fe^{3+} in solution as another endmember case.

In nature, this endmember case may be rare. One likely example is pure ZnS oxidation by Fe^{3+}. Pure ZnS is acid-soluble, and its oxidation process was proposed to proceed entirely in solution (Moses et al. 1987). The $\Delta\delta^{18}O_{SO_4-H_2O}$ obtained in pure ZnS oxidation via Fe^{3+} experiments is 8.2‰ (Balci et al. 2012), which is close to the 5.9‰ obtained from sulfite oxidation by Fe^{3+} in solution (Müller et al. 2013a). The 2.3‰ difference could arise from the different sulfite and Fe^{3+} concentrations and Fe^{3+}/sulfite ratios in the two experiments. The concentration difference may affect the oxidation kinetics (Lente and Fábián 2002) and consequently, the oxygen isotope fractionations.

As discussed in the section above, sulfite should have maintained its oxygen isotope equilibrium with water at low pH conditions. Thus, the oxygen isotope composition of sulfate derived from sulfite oxidation by Fe^{3+} in solution can be calculated by,

$$^{17,18}R_{SO_4^{2-}}^{D.F.I.} = \left(\frac{3}{4} {}^{17,18}KIE_{SO_3^{2-}/Fe^{3+}\rightarrow SO_4^{2-}} {}^{17,18}\alpha_{SO_3^{2-}-H_2O}^{EQ} + \frac{1}{4} {}^{17,18}KIE_{H_2O\rightarrow SO_4^{2-}} \right) {}^{17,18}R_{H_2O} \quad (17)$$

The related kinetic and equilibrium triple isotope effects will be constrained by Monte Carlo technique later.

The role of microbes on oxygen isotope composition of sulfate derived from sulfur oxidation

Microbial enzymatic processes affect sulfate oxygen isotopes during sulfur oxidation. Two metabolic mechanisms can be identified (Fig. 3). One catalyzes the Fe^{2+} oxidation to Fe^{3+} with O_2 as the ultimate electron acceptor at low pH conditions and the product Fe^{3+} in turn oxidizes sulfur abiotically (Fig. 3a) (Singer and Stumm 1970; Balci et al. 2007; Brunner et al. 2008). The other catalyzes direct sulfur oxidation in which both Fe^{3+} and O_2 can act as oxidants (Fig. 3b) (McCready and Krouse 1982; Sand et al. 1995; Balci et al. 2012). Note that these two mechanisms often work jointly (Schippers et al. 1996; Brunner et al. 2008; Vera et al. 2013), and no clear boundary exists for this division. In fact, even for enzyme-mediated direct sulfur oxidation, there are different enzymatic pathways involved (Fig. 4), including sulfite oxidation through sulfite dehydrogenase (Feng et al. 2007) or APS (Kelly 2003), tetrathionate hydrolysis (Ghosh and Dam 2009), and Sox reactions (Friedrich et al. 2001). Therefore, multiple oxidation pathways compete when microbes are participating in sulfur oxidation processes. Oxygen isotope exchange between intermediates and water, substrates used by enzymes, and the reversibility of enzymatic reactions could all influence the oxygen isotope composition of the final sulfate. Experiments targeted at individual variables are scarce at this time. As a result, these multiple, interacting factors make a quantitative prediction difficult on the oxygen isotopes of sulfate derived from microbial oxidation. However, some general conclusions on the role of microbes in sulfate oxygen isotopes during oxidation can be drawn.

Balci et al. (2007) found that their microbial anaerobic (Fe^{3+} as the oxidant) and aerobic (O_2 as the oxidant) long-term pyrite oxidation experiments resulted in similar $\Delta\delta^{18}O_{SO_4-H_2O}$. Their interpretation is that Fe^{3+} is the direct oxidant in their experiments, even when O_2 is the ultimate electron acceptor in the aerobic experiments. Their later ZnS and S oxidation experiments (Balci et al. 2012) support the interpretation. If correct, microbes appear to catalyze Fe^{2+} oxidation by O_2, which diminishes the fraction of O_2 signature being incorporated in product sulfate (Fig. 3a).

When sulfur is oxidized directly via microbial enzymatic reactions and sulfite–water oxygen isotope equilibrium is maintained, sulfite dehydrogenase pathway may have a similar oxygen isotope effect as does the sulfite oxidation by Fe^{3+} (Fig. 4), in which the $\Delta\delta^{18}O_{SO_4-H_2O}$ is ~ 8‰. Sulfite oxidation through APS (Fig. 4) is expected to be similar to microbial sulfate reduction (Fig. 2), which can result in a $\Delta\delta^{18}O_{SO_4-H_2O}$ value at 14.8‰~28‰ depending on reaction reversibility. However, this pathway may not be highly expressed during sulfur oxidation (Klatt and Polerecky 2015). If tetrathionate can reach oxygen isotope equilibrium with water, tetrathionate hydrolysis (Fig. 4) will have a similar isotope effect, as does thiosulfate oxidation on pyrite surface i.e., about 2.6‰. However, existing experimental results indicate that the rate of oxygen isotope exchange between tetrathionate and water is slow compared with the rate of tetrathionate hydrolysis (Balci et al. 2017). Sox pathway has variable substrates, e.g., SO_3^{2-}, S^{2-}, and $S_2O_3^{2-}$ (Fig. 4). When sulfite is the substrate, the corresponding isotope effect is expected to be similar to that for thiosulfate oxidation on the pyrite surface, i.e., about 2.6‰. When S^{2-} is the substrate, four oxygen addition steps are required to produce sulfate.

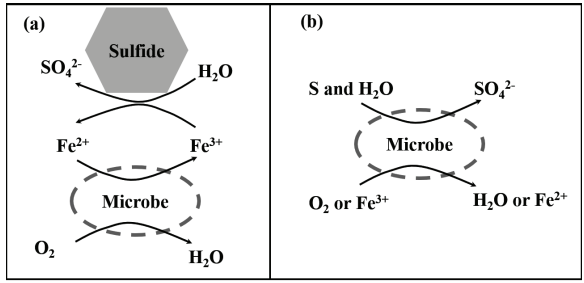

Figure 3 Two endmember metabolic mechanisms (a and b), yet often working jointly, affect oxygen isotope composition of sulfate derived from sulfur oxidation. The **grey dashed circles** mark the cell membrane. **Black arrows** indicate the reaction path from reactants to products.

Sulfite dehydrogenase pathway:

$$\mathbf{SO_3^{2-}} + 2(Fe^{3+})\ \text{cytochrome c} + \mathbf{H_2O} \rightarrow \mathbf{SO_4^{2-}} + 2(Fe^{2+})\ \text{cytochrome c} + 2H^+$$

APS pathway:

$$\mathbf{AMP} \xrightarrow{\mathbf{SO_3^{2-}}} \mathbf{APS} \xrightarrow{PP_i} ATP + \mathbf{SO_4^{2-}}$$

Tetrathionate hydrolysis pathway:

$$O_3S_3\mathbf{SO_3^{2-}} + \mathbf{H_2O} \rightarrow S_2O_3^{2-} + \mathbf{SO_4^{2-}} + S^0 + 2H^+$$

Sox pathway:

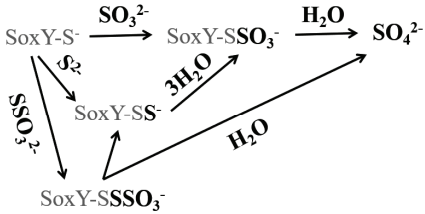

Figure 4. Enzyme-catalyzed sulfur oxidation pathways. The substrates can be SO_3^{2-} (Kelly 2003; Feng et al. 2007), $S_4O_6^{2-}$ (Ghosh and Dam 2009), S^{2-} (Friedrich et al. 2001), or $S_2O_3^{2-}$ (Friedrich et al. 2001), respectively; these substrates may or may not readily exchange oxygen with water during oxidation; the added oxygens to these substrates are exclusively from water. Chemical compounds marked with bold black are sulfur and oxygen sources in product sulfate.

If these steps are irreversible and oxygen isotope exchange rates between the intermediates and water are relatively slow, a negative $\Delta\delta^{18}O_{SO_4-H_2O}$ value is expected due to kinetic isotope effects. Negative $\Delta\delta^{18}O_{SO_4-H_2O}$ observed in elemental sulfur oxidation by *A. thiooxidans* (Smith et al. 2012; Balci et al. 2017) may indicate the operation of a Sox pathway. When SSO_3^{2-} is the substrate, the $\Delta\delta^{18}O_{SO_4-H_2O}$ is expected to have a value in between the ones where SO_3^{2-} and S^{2-} are substrates, respectively, since the oxidation of SSO_3^{2-} can be regarded as the oxidation of SO_3^{2-} and S^{2-} continuously via Sox pathway (Fig. 4). However, we should note that these rough estimations are only for specific oxidation pathway instead of for specific microbial community because one community may operate multiple oxidation pathways at the same time (Bobadilla Fazzini et al. 2013). Because most of these microbial mediated sulfur oxidation steps are physically separated from O_2 reduction steps by specific enzymes (Kelly 1982; Balci et al. 2017), the chance for O_2 to be directly bonded to S and eventually to product sulfate is low.

In summary, the overall impact of microbial involvement in sulfate production via sulfur oxidation is a reduction of the proportion of O_2 isotope signal that could otherwise be incorporated in sulfate if oxidation occurs abiotically.

Comments on laboratory experiments

While the results on oxygen isotope effects from the published sulfur oxidation experiments generally converge, discrepancies and uncertainties exist. Knowing these caveats help to scrutinize data for our prediction for sulfate endmembers in $\Delta'^{17}O$–$\delta^{18}O$ space later.

Most of abiotic, aerated pyrite oxidation experiments show that less than 15% of the oxygen in product sulfate is sourced from O_2 (Taylor et al. 1984a; Balci et al. 2007; Heidel et al. 2009; Tichomirowa and Junghans 2009; Heidel and Tichomirowa 2010), while Kohl and Bao (2011)'s experiments show that more than 20% oxygen in sulfate is derived from O_2 even with Fe^{3+} added. We infer that strong hydrodynamics brought about by constant shaking in Kohl and Bao's experiments may have enhanced the release of thiosulfate into solutions, which increases O_2 incorporation in product sulfate. Also, Tichomirowa and Junghans (2009)'s and Heidel et al. (2009)'s experiments indicate that smaller pyrite grain size (e.g., smaller than 63 μm) increases the release of thiosulfate and therefore also the O_2 fraction in sulfate.

Pyrite oxidation experiments show that the duration of aerobic experiments (Tichomirowa and Junghans 2009) and Fe^{3+}/surface ratio of anaerobic experiments (Heidel and Tichomirowa 2011) affect sulfate oxygen isotope composition. Both factors point to the importance of thoroughly washing clean pyrite grains before the experiment. Sulfate initially presented on sulfide mineral surface is often difficult to eliminate, and a long experimental duration may be required to overwhelm this "background" sulfate. A higher fraction of O_2 signal in sulfate collected at the beginning of an experiment (Balci et al. 2007; Heidel et al. 2009; Tichomirowa and Junghans 2009; Heidel and Tichomirowa 2010; Ziegler et al. 2010) may be explained by this high "background".

Most laboratory experiments on pyrite oxidation were conducted at pH ~ 2 (Taylor et al. 1984a; Balci et al. 2007; Mazumdar et al. 2008; Tichomirowa and Junghans 2009; Heidel and Tichomirowa 2011). In Kohl and Bao (2011) some of the pyrite oxidation experiments were carried out in solutions buffered at higher pH conditions in which negative $\Delta\delta^{18}O_{SO_4-H_2O}$ were observed, indicating that sulfite, the assumed intermediate, probably did not reach oxygen isotope equilibrium with the water. We calculated, based on Equation (9), that sulfite–water oxygen isotope exchange rate is at ~9×10^{-5}, 9×10^{-7}, and 9×10^{-9} s^{-1} at pH 9, 10, and 11, respectively. These rates are slower than the oxidation rates at pH 9 and 10 in the initial 10–20 weeks, and also slower than that at pH 11 at all times, according to Kohl and Bao (2011). Therefore, sulfate–water oxygen isotope fractionation at acidic conditions does not apply to cases at alkaline conditions. In addition, the pH buffered solution may affect the pyrite oxidation process. For example, the fraction of O_2 signal in sulfate decreased at pH 10 and 11 when compared to the acidic conditions even without the addition of Fe^{3+} ion. A possible explanation is that carbonate ion in the buffered solution accelerates the oxidation of Fe^{2+} to Fe^{3+} when pyrite is oxidized in aerated solution (Caldeira et al. 2010) which enhances iron's reactivity. Likewise, the fraction of the O_2 signal in sulfate is higher at pH 7 even with Fe^{3+} addition than at other pH conditions. A possible explanation is that phosphate in the buffered solution was precipitated with Fe^{2+} and Fe^{3+} as solids (Nriagu 1972; Singer 1972), resulting in a reduced iron's reactivity in solution.

The concentration of sulfite, the most important intermediate during sulfur oxidation, as well as sulfite/oxidant ratio, can affect the rate of oxidation (Lente and Fábián 2002), and therefore the $\Delta\delta^{18}O_{SO_4-H_2O}$. This can explain why different oxygen isotope effects were observed in the similar sulfite oxidation experiments by O_2 (Oba and Poulson 2009; Müller et al. 2013a) or among experiments of sulfite, ZnS, and S oxidation by Fe^{3+} (see section *Sulfite oxidation by Fe^{3+} in solution*).

It was observed that ~40% of the oxygen in sulfate derived from copper-catalyzed aerated oxidation of sulfite is sourced from O_2 (Holt et al. 1981). We think this explains the 43% O_2-sourced oxygen in sulfate derived from the chalcopyrite abiotic oxidation experiments conducted by Thurston et al. (2010). It also explains the 8% O_2-sourced oxygen in sulfate derived from pyrite and pure ZnS microbial oxidation experiments conducted by Balci et al. (2007, 2012). In Balci et al.'s experiments, $CuCl_2$ was added in their microbial culture medium. Further examination of the role of copper ion is warranted.

Constraining intrinsic equilibrium and kinetic oxygen isotope effects during sulfide oxidation

We need the EIEs and KIEs to predict the $\Delta'^{17}O$–$\delta^{18}O$ space for endmember sulfates quantitatively. These intrinsic isotope effects can be obtained by examining the published experimental data. The knowledge synthesized in the previous sections allows us to avoid potentially messy and misleading data while focusing on the $\Delta\delta^{18}O_{SO_4-H_2O}$ values obtained from abiotic experiments that were conducted in acidic conditions with a sufficiently long duration.

Let us begin by considering the KIE and EIE for sulfite oxidation by O_2 in solution. Here we use Monte Carlo technique, an approach we have applied to analyze methane KIEs (Cao et al. 2019), to constrain the values of $KIE_{SO_3/O_2\rightarrow SO_4}$, $\alpha^{EQ}_{SO_3^{2-}-H_2O}$, and $KIE_{O_2\rightarrow SO_4}$ in Equation (16). Results from laboratory-controlled aerobic pyrite oxidation experiments at pH 2 (Tichomirowa and Junghans 2009; Kohl and Bao 2011), in which about 25% oxygen in sulfate was found to come from O_2, were used as input constraints. We used 24.2‰ as the $\delta^{18}O$ for dissolved O_2 (Kroopnick and Craig 1972; Reuer et al. 2007; Li et al. 2019). We obtained values of $KIE_{SO_3/O_2\rightarrow SO_4}$, $\alpha^{EQ}_{SO_3^{2-}-H_2O}$, and $KIE_{O_2\rightarrow SO_4}$ in Equation (16) at 0.9916 ± 0.0003, 1.0129 ± 0.0001, and 0.9850 ± 0.0010, respectively (Table 1). The determined KIE for sulfite is close to the experimentally determined 0.9903 by Muller et al (2013a). The $\alpha^{EQ}_{SO_3^{2-}-H_2O}$ of 1.0129 is within the range of 7.9‰ and 15.2‰ fractionation determined experimentally (Brunner et al. 2006; Müller et al. 2013b; Wankel et al. 2014). The determined $KIE_{O_2\rightarrow SO_4}$ of 0.9850 is, however, rather different from 0.997 (Oba and Poulson 2009) and 1.007 (Müller et al. 2013a) determined experimentally through sulfite oxidation by O_2. It should be noted that the Monte Carlo method determines possible EIE and KIE solutions and their probability. The isotope effects presented above are the most likely solutions under given constraints. The results can be changed when some of the parameters are constrained to be different in the future.

Experimental results from the abiotic ZnS oxidation by Fe^{3+} (Balci et al. 2012) are chosen to represent an endmember case of sulfite oxidation by Fe^{3+} in solution. Instead of linear regression used by Balci et al. (2012), the oxygen isotope composition in water and sulfate, as depicted by Equation (17), is used here directly to calculate the apparent $\alpha_{SO_4-H_2O}$, which is determined to be 1.0079 ± 0.0009. If $\alpha^{EQ}_{SO_3^{2-}-H_2O}$ is assumed to be 1.0129, $KIE_{SO_3/Fe^{3+}\rightarrow SO_4}$ and $KIE_{H_2O\rightarrow SO_4}$ are determined to be 0.9984 ± 0.0008 and 0.9976 ± 0.0014, respectively by Monte Carlo method (Table 1). Again, these values are the most probable solutions for the observed sulfate–water oxygen isotope fractionation, and further constraints can revise and improve these values.

Abiotic anaerobic oxidation of pyrite conducted by Balci et al. (2007), Mazuzumdar et al. (2008), and Heidel and Tichomirowa (2011) are chosen here to represent the endmember case of thiosulfate oxidation by Fe^{3+} on pyrite surface. Sulfate–water oxygen isotope fractionation is calculated to be 1.0027 ± 0.0007 using Equation (15). If $\alpha^{EQ}_{SSO_3^{2-}-H_2O}$ and $KIE_{H_2O\rightarrow SO_4}$ are set to be 1.0129 and 0.9976, respectively, $KIE_{SSO_3\rightarrow SO_4}$ is estimated to be 0.9916 ± 0.0005 (Table 1).

The θ values for the many important KIEs during sulfide oxidation are underconstrained for now. If reduced masses, i.e., imaginary frequency term in transition state (Young et al. 2002; Bao et al. 2015), are used to calculate the values of θ for these KIEs, the range is 0.5052–0.5168 (Table 1). Lower θ_{KIE} values are associated with thiosulfate or sulfite, while higher values are obtained for H_2O and O_2. However, the exact θ_{KIE} values cannot be determined at this time. An arbitrary value of 0.5110, i.e., the mean of the maximum (0.5168) and minimum (0.5052) θ_{KIE} in Table 1, will be used for discussion hereafter.

Table 1. Constrained intrinsic or diagnostic KIE, EIE, and θ values for sulfide oxidation processes. The $^{18}\alpha^{EQ}_{SO_4^{2-}-H_2O}$ is calculated at 25 °C based on Equation (6); $^{18}\alpha^{EQ}_{SO_3^{2-}-H_2O}$ and KIEs are determined by Monte Carlo method. $^{18}\alpha^{EQ}_{SSO_3^{2-}-H_2O}$ is assumed to equal to $^{18}\alpha^{EQ}_{SO_3^{2-}-H_2O}$; θ_{RM} refers to θ value determined using reduced masses of associated reactants; The θ values for $^{18}\alpha^{EQ}_{SO_4^{2-}-H_2O}$, $^{18}\alpha^{EQ}_{SO_3^{2-}-H_2O}$, and $^{18}\alpha^{EQ}_{SSO_3^{2-}-H_2O}$ are set at 0.524 based on the value of $\theta^{EQ}_{SM-H_2O}$ (see section *Sulfoxyanions–water oxygen isotope exchange*); The θ value for all KIEs is set to 0.511 which is equal to the mean value of maximum and minimum θ_{RM}.

	Values of EIE/KIE	θ_{RM} values[e]	θ values
$^{18}\alpha^{EQ}_{SO_4^{2-}-H_2O}$	1.023	--	0.524[g]
$^{18}\alpha^{EQ}_{SO_3^{2-}-H_2O}$[a]	1.0129 ± 0.0001	--	0.524
$^{18}\alpha^{EQ}_{SSO_3^{2-}-H_2O}$	1.0129 ± 0.0001	--	0.524
$KIE_{O_2\rightarrow SO_4}$[b]	0.9850 ± 0.0010	0.5109	0.511
$KIE_{SO_3/O_2\rightarrow SO_4}$[c]	0.9916 ± 0.0003	0.5064	0.511
$KIE_{H_2O\rightarrow SO_4}$[d]	0.9976 ± 0.0014	0.5168/0.5161[f]	0.511
$KIE_{SO_3/Fe^{3+}\rightarrow SO_4}$[d]	0.9984 ± 0.0008	0.5067	0.511
$KIE_{SSO_3\rightarrow SO4}$	0.9916 ± 0.0005	0.5052	0.511

a: $^{18}\alpha^{EQ}_{SO_3^{2-}-H_2O}$ was determined to be about 1.008 (Brunner et al. 2006), 1.009 (Wankel et al. 2014), and 1.015 (Müller et al. 2013b), respectively; **b:** $KIE_{O_2\rightarrow SO_4}$ was determined to be ~ 0.997 (Oba and Poulson 2009) and 1.007~1.023 (Müller et al. 2013a), respectively; **c:** $KIE_{SO_3/O_2\rightarrow SO_4}$ was determined to be ~ 0.990~0.995 (Müller et al. 2013a); **d:** $3/4 \times KIE_{SO_3/Fe^{3+}\rightarrow SO_4} + 1/4 \times KIE_{H_2O\rightarrow SO_4}$ was determined to be ~ 0.994 (Müller et al. 2013a); **e:** $\theta_{RM} = \ln(^{17}\mu/^{16}\mu)/\ln(^{18}\mu/^{16}\mu)$, where μ is the reduced mass of associated reactants, e.g. O_2 and SO_3^{2-}; **f:** 0.5168 and 0.5161 are for sulfite and thiosulfate oxidation processes, respectively; **g:** the value of 0.524 was taken from the θ values for sulfate minerals-water determined by Schauble and Young (2021, this volume).

APPLICATIONS

As shown in Equations (13) and (15–17), given the triple oxygen isotope compositions of water and O_2 and the constrained KIEs, EIEs, and θs, we can predict the values of $\delta^{18}O$ and small $\Delta'^{17}O$ for endmember sulfate identified above. The predicted results can be compared with field observations. Because the triple oxygen isotope compositions of water and O_2 of the geological past are not well constrained, we will only explore the small $\Delta'^{17}O_{SO_4}$ in modern sulfate. Specifically, modern sulfate from Ace lake in Antarctica and Mississippi and Marsyangdi river basins will be analyzed.

Predicted sulfate $\delta^{18}O$ and small $\Delta'^{17}O$

Let us first set the triple oxygen isotope compositions of water and dissolved O_2 that are required to make the prediction. The meteoric water is assumed to be on the Global Meteoric Water Line (GMWL) (Luz and Barkan 2010),

$$\delta'^{17}O = 0.528 \times \delta'^{18}O + 0.000033 \quad (18)$$

and we will use the range of −20‰ to 0‰ for $\delta^{18}O_{H_2O}$ with a corresponding $\delta^{17}O_{H_2O}$ calculated using Equation (18). For dissolved O_2, we use fixed $\delta^{18}O$ and $\Delta'^{17}O$ at 24.2‰ and −0.554‰, respectively (Kroopnick and Craig 1972; Reuer et al. 2007; Barkan and Luz 2011; Li et al. 2019).

Using the constrained endmember triple oxygen isotope parameters in Table 1 and Equations (13, 15–17), we have constructed sulfate $\Delta'^{17}O$–$\delta^{18}O$ space for four different endmember cases given the range of $\delta^{18}O_{H_2O}$ (Fig. 5). The results show that sulfate $\Delta'^{17}O$ is apparently negatively correlated with its $\delta^{18}O$. Sulfate derived from surface oxidation has the most positive $\Delta'^{17}O$ values. Its $\Delta'^{17}O$ can be even more positive than that of its ambient water. As graphically illustrated in Figure 6a, the combination of EIE and KIEs during sulfide oxidation can produce

a diagnostic $\theta_{SO_4-H_2O}$ value higher than 0.5305. Comparing with Figure 6c, Figure 6a shows that a smaller $KIE_{SSO_3\rightarrow SO_4}$ (i.e., $\ln(KIE_{SSO_3\rightarrow SO_4})$ being more negative than $\ln(KIE_{SO_3/Fe^{3+}\rightarrow SO_4})$, see Table 1) associated with thiosulfate oxidation to sulfate on pyrite surface is the key to achieve a diagnostic $\theta_{SO_4-H_2O}$ value larger than 0.5305. Interestingly, the $\Delta'^{17}O$ of sulfate derived from solution oxidation by dissolved O_2 is only slightly more negative than that of the water, even though 25% oxygen of this sulfate is derived from O_2, which carries a $\Delta'^{17}O$ of –0.554‰ to begin with. Figure 6b shows that the negative $\Delta'^{17}O$ signal in O_2 is largely erased by its KIE when O_2 is incorporated into the sulfate. The $\Delta'^{17}O$ value of sulfate derived from solution oxidation by Fe^{3+} (Fig. 6c) is even more negative than that derived from the O_2 oxidation pathway (Fig. 6b). The most negative $\Delta'^{17}O$ value is possessed by the equilibrated sulfate (Figs. 5 and 6d), attributed largely by its more positive $\delta^{18}O$ value riding on a θ^{EQ} value smaller than the reference 0.5305. All these results highlight the importance of knowing the intrinsic isotope effects during sulfate formation when a small sulfate $\Delta'^{17}O$ is of interest, and isotopologue specific kinetic analysis is critical to correctly interpreting small $\Delta'^{17}O$.

The distinct curves in Figure 5 demonstrate that sulfate $\delta^{18}O$ and $\Delta'^{17}O$ can be used to differentiate sulfate of different oxidation origins. The distribution of curves also reveals that sulfates derived from the two solution oxidation pathways, by O_2 and by Fe^{3+}, are difficult to tell apart. Since the Fe^{3+} path is only dominant in very acidic conditions such as acid mine drainages because Fe^{3+} precipitates at higher pH (Stefánsson 2007), its geological significance is, therefore, limited. However, we should note that the results presented in Figure 5 are obtained according to our best estimations for the intrinsic or diagnostic EIEs and KIEs presented in Table 1. When the values of these EIEs and KIEs are further constrained to be different sulfate $\delta^{18}O$ and $\Delta'^{17}O$ should be changed accordingly.

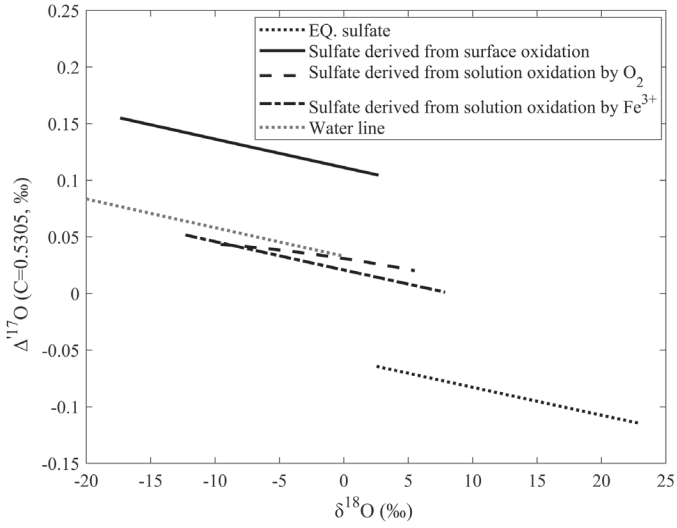

Figure 5. Triple oxygen isotope compositions of sulfate derived from different mechanisms in a given water body. The value of $\delta^{18}O_{H_2O}$ is set to range from –20‰ to 0‰ with the corresponding $\delta^{17}O_{H_2O}$ being estimated by Equation (18); "EQ. sulfate" refers to sulfate at oxygen isotope equilibrium with water; "sulfate derived from surface oxidation" refers to the endmember from thiosulfate oxidation on pyrite surface; "sulfate derived from solution oxidation by O_2" refers to the endmember from sulfite oxidation by O_2 in solution; "sulfate derived from solution oxidation by Fe^{3+}" refers to the endmember from sulfite oxidation by Fe^{3+} in solution; EIEs, KIEs, and their corresponding θs presented in Table 1 are used to determine the triple oxygen isotope compositions in these endmember sulfates. "Water line" indicates global meteoric water line.

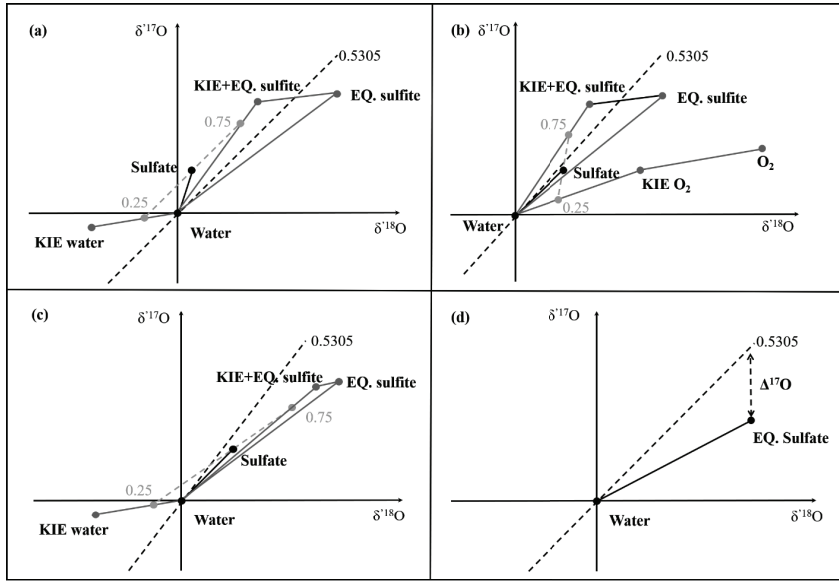

Figure 6. Schematic illustration of the generation of small $\Delta'^{17}O$ in sulfate derived from four different end-member cases. Water is at the **origin**, and the **black dashed line** is the reference line going through the origin with a slope of 0.5305. "EQ. sulfite" and "EQ. sulfate" refer to the sulfite and sulfate when at oxygen isotope equilibrium with water, respectively; "KIE + EQ. sulfite", "KIE O_2", and "KIE water" mark the triple oxygen isotope compositions of sulfite, O_2, and water when they are incorporated into sulfate, respectively; The number "0.25" means that 25% oxygen of sulfate sourced from "KIE water" or "KIE O_2", respectively, and "0.75" means that 75% oxygen of sulfate sourced from "KIE + EQ. sulfite". The **black dot** "sulfate" located at the middle of a **grey dashed line** connecting "0.25" and "0.75"is where the final product sulfate sits in $\Delta'^{17}O$–$\delta^{18}O$ space. The slope of a **solid grey line** marks specific equilibrium, kinetic, or apparent θs.

Lake sulfate

Ace lake, Antarctica, is a meromictic lake with an active microbial sulfur cycling (Burton and Barker 1979; Lauro et al. 2011). Two sulfate samples, from a depth of 5.5 m and 15.5 m, respectively, have been measured for their $\delta^{34}S$, $\delta^{18}O$ and $\Delta'^{17}O$ (Fig. 7) (Sun et al. 2015). The water temperatures were ~ 1 °C and ~ 3 °C, respectively, for these two samples (Lauro et al. 2011), and $\delta^{18}O_{H_2O}$ value was ~ −16.7‰ (Sun et al. 2015). The observed apparent $\Delta\delta^{18}O_{SO_4\text{–}H_2O}$ is, therefore, 25.2 ± 0.7‰ at 15.5 m (Fig. 7), which is very close to the equilibrium $\Delta\delta^{18}O_{SO_4\text{–}H_2O}$ value of 27.2‰ calculated at 3 °C based on Equation (6). This similarity suggests that sulfate and water have probably reached oxygen isotope equilibrium at 15.5 m in this permanently stratified lake. Given the measured $\delta^{18}O$ and $\delta^{17}O$ of sulfate and assuming a $\theta_{SO4\text{-}H2O}^{EQ}$ of 0.524, we determined that the $\Delta'^{17}O$ in water is −0.146 ± 0.043‰. A negative $\Delta'^{17}O_{H2O}$ suggests a highly evaporated water body (Surma et al. 2015; Gázquez et al. 2018; Passey and Ji 2019), as is likely the case based on Ace lake water history (Roberts et al. 1999). At 5.5 m, the apparent $\Delta\delta^{18}O_{SO_4\text{–}H_2O}$ is 20.0 ± 0.7‰ which is much smaller than $\Delta\delta^{18}O_{SO_4\text{–}H_2O}^{eq}$, i.e., 27.7‰ at 1 °C, suggesting that sulfate and water are not in oxygen isotope equilibrium at this shallower depth (Fig. 7). Given the lake water oxygen isotope composition, we calculated the apparent θ for sulfate of the MSR pathway, θ_{MSR}^{app}, to be at 0.5288 ± 0.0028, which is higher than the equilibrium θ value of 0.524 we concluded earlier and close to the θ_{MSR} value of 0.5285 ± 0.0026 estimated by Waldeck et al. (2019). These data suggest that the non-equilibrium MSR processes possess higher θ values than a sulfate–water equilibrium system. The case of Ace Lake sulfate illustrates the potential of using small $\Delta'^{17}O$ in sulfate to constrain sulfur cycling in lake systems and lake water triple oxygen isotope compositions.

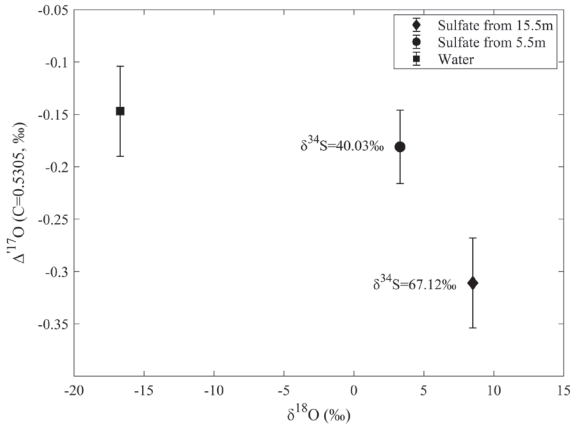

Figure 7. Oxygen and sulfur isotope compositions in sulfate from two different depths in Ace Lake, Antarctica. The large $\delta^{18}O$ difference between sulfate and water at 15.5 m, i.e., 25.2 ± 0.7‰, suggests sulfate and water may have achieved oxygen isotope equilibrium.

Riverine sulfate

Mississippi river sulfate. Killingsworth et al. (2018) presented a four-year monthly to biweekly $\delta^{34}S$, $\delta^{18}O$, and $\Delta'^{17}O$ dataset for sulfate from Mississippi River Basin (MiRB). The four-year average values of $\delta^{18}O_{SO_4}$ and $\Delta'^{17}O_{SO_4}$ are 3.4‰ and −0.09‰, respectively. Given an average $\delta^{18}O_{H_2O}$ value of −6.6‰ for MiRB (Killingsworth et al. 2018), if the sulfate were all derived from thiosulfate oxidation on pyrite surface, we would predict a $\delta^{18}O_{SO_4}$ of −3.9‰. If the sulfate were all derived from sulfite oxidation by O_2 in solution, we would anticipate a $\delta^{18}O_{SO_4}$ of 0.5‰. Both predicted endmember $\delta^{18}O_{SO_4}$ values are lower than the observed average $\delta^{18}O_{SO_4}$ of 3.4‰. From the $\delta^{34}S_{SO_4}$ data and considering the contribution of sulfate from evaporite source, Killingsworth et al. (2018) estimated the fraction of pyrite derived sulfate in MiRB to be ~72%. Given this percentage and evaporite $\delta^{18}O_{SO_4}$ of 10‰ to 20‰ (Calmels et al. 2007), we estimate sulfate derived from sulfide oxidation in MiRB would have a $\delta^{18}O$ value of 0‰ to 2.8‰ or 3.2‰ to 6.0‰ if pyrite oxidation is through thiosulfate oxidation on pyrite surface or sulfite oxidation by O_2 in solution, respectively. These estimates offer no information on the relative dominance of either of the endmember pyrite oxidation pathways in MiRB due to their close $\delta^{18}O$ values. However, the small $\Delta'^{17}O_{SO_4}$offers a better resolution to this distinction. We estimate that the $\Delta'^{17}O_{SO_4}$ for surface and solution oxidation are 0.121‰ and 0.030‰, respectively (Fig. 5). Using a $\Delta'^{17}O$ of −0.057‰ for evaporite sulfate (Cowie and Johnston 2016) and the 72% fraction of pyrite derived sulfate, the $\Delta'^{17}O$ of MiRB sulfate should be 0.071‰ and 0.006‰, respectively, for the surface and solution oxidation endmembers. Obviously, both values are higher than the observed value of −0.09‰. The observed more negative $\Delta'^{17}O$ in MiRB sulfate is not likely caused by MSR process (Hemingway et al. 2020) because MSR can increase $\delta^{18}O_{SO_4}$ at the same time, which is not observed. One reason for this apparent discrepancy is that the measured $\Delta'^{17}O_{SO_4}$ in the Mississippi river sulfate is more negative than its real value due to the partial yield of O_2 during laser fluorination. The data of $\Delta'^{17}O_{SO_4}$ in Killingsworth et al. (2018) were measured at Bao's laboratory at Louisiana State University. Comparing Bao et al.'s NBS 127 $\Delta'^{17}O_{SO_4}$value to the one determined by Cowie et al. in Johnston's laboratory (Bao and Thiemens 2000; Cowie and Johnston 2016), Cowie et al.'s $\Delta'^{17}O_{SO_4}$ is ~0.088‰ (or ~0.07‰, personal communication with David Johnston) higher than the one obtained by Bao et al. If this 0.088‰ (or 0.07‰) is added to Killingsworth et al.'s measured $\Delta'^{17}O_{SO_4}$ data, the averaged $\Delta'^{17}O_{SO_4}$ will be −0.002‰ (or −0.02‰), which matches

well with the pathway of sulfite oxidation by O_2 in solution. However, this agreement might be fortuitous because $\Delta'^{17}O_{SO_4}$ for seawater sulfate measured in Bao's lab and Johnston's lab is almost identical, i.e., ~ −0.01‰ (Bao and Thiemens 2000; Cowie and Johnston 2016). In addition, the average MiRB $\Delta'^{17}O_{H_2O}$ may be off the GMWL given by Equation (18) (Li et al. 2015; Sharp et al. 2018; Bindeman et al. 2019), and there are uncertainties in our estimated EIE and KIE values and their corresponding θs. Nevertheless, this specific case reveals that small $\Delta'^{17}O_{SO4}$ can add additional constraints on the origin of riverine sulfate, although further calibration work is required to substantiate and expand this utility.

Marsyangdi river sulfate. Hemingway et al. (2020) presented a $\delta^{18}O$ and $\Delta'^{17}O$ data set for sulfate from Marsyangdi River Basin (MaRB), Nepal. Remarkably, some of the upper-valley sulfates have $\Delta'^{17}O$ values as positive as 0.18‰, even more positive than the one estimated for the ambient water. Pyrite oxidation by atmospheric H_2O_2 was proposed to interpret the rather positive $\Delta'^{17}O_{SO_4}$ values (Hemingway et al. 2020). However, it is not clear how H_2O_2 is delivered to the pyrite oxidation site (Hemingway et al. 2020). From our analysis (Fig. 8), a positive $\Delta'^{17}O_{SO_4}$ can be achieved if sulfate is derived from thiosulfate oxidation on the pyrite surface. Using the measured water isotope data, we estimate this endmember sulfate's $\delta^{18}O$ and $\Delta'^{17}O$ at −12.1‰ and 0.14‰, respectively. Both of them are in close agreement with the observed ones (Fig. 8). The discrepancy between our predicted 0.14‰ and the highest observed 0.18‰ may result from uncertainties associated with the $\Delta'^{17}O$ of ambient water, EIE and KIE, and their respective θ values.

MaRB $\Delta'^{17}O_{SO_4}$ decreases toward downstream and microbial sulfate reduction and reoxidation are proposed as the cause (Hemingway et al. 2020). This interpretation is comparable to the Ace lake case where MSR processes are shifting sulfate oxygen isotope composition toward equilibrium (Fig. 8).

ANALYTICAL METHODS

O_2 is the gaseous analyte for accurate triple oxygen isotope analysis due to its minimal isobaric interference. Other gases, e.g., CO_2, CO, or SO_2, certainly cannot deliver a $\Delta'^{17}O$ uncertainty down to ±0.01‰ required in studying small $\Delta'^{17}O$ variations, e.g., from −0.3 to +0.3‰. O_2 generation from sulfate is done by converting SO_4^{2-} ion into a solid form, either $BaSO_4$ or Ag_2SO_4. The powdery sulfate solids can be fluorinated (Bao and Thiemens 2000; Bao 2006; Cowie and Johnston 2016) or in the case of Ag_2SO_4 thermally decomposed (Savarino et al. 2001; Schauer et al. 2012; Geng et al. 2013) to generate O_2. Sample purification is important during the precipitation of solid sulfate from the solution because other oxygen-bearing compounds can be incorporated into $BaSO_4$ or Ag_2SO_4. When the sample size is not an issue, $BaSO_4$ is the recommended solid to work with. $BaSO_4$ is easy to handle and to be purified using a chelating method (Bao 2006).

One important caveat in generating O_2 from sulfate solids is that O_2 yield is not quantitative, ranging from 20–35% (Bao and Thiemens 2000) to 50% (Cowie and Johnston 2016) when BrF_5 and F_2 vapor are used in laser fluorination, respectively. The partial O_2 yield results in the raw $\delta^{18}O$ value being 8‰ to 20‰ lower than the true $\delta^{18}O$ value we separately obtain by analyzing CO gas generated by an online Temperature-conducive elemental analyzer connected to an isotope-ratio mass spectrometer (IRMS). We calculate the $\Delta'^{17}O$, however, using the raw $\delta^{18}O$ and $\delta^{17}O$ measured simultaneously in dual-inlet model on an IRMS. This is hardly an issue when a large sulfate $\Delta'^{17}O$ is of interest. However, a small sulfate $\Delta'^{17}O$ value is sensitive to both the $\delta^{18}O$ value and the triple oxygen isotope exponent of the reaction that generates the partial O_2 yield. Laboratory tests show that the $\Delta'^{17}O$ from three ~10% aliquots of O_2 generated

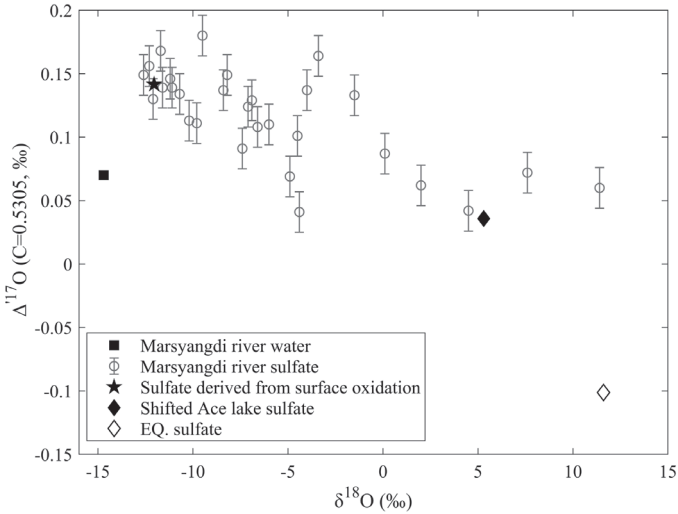

Figure 8. Triple oxygen isotope compositions of Marsyangdi River Basin sulfate and sulfate of different endmember pathways. The value of $\Delta'^{17}O$ in "Marsyangdi river water" is estimated by Equation (18); triple oxygen isotope compositions in "Marsyangdi river sulfate" is from Hemingway et al. (2020); "Sulfate derived from surface oxidation" refers to the endmember from thiosulfate oxidation on pyrite surface, and EIE, KIEs, and their corresponding θs presented in Table 1 are used to determine its triple oxygen isotope compositions; triple oxygen isotope composition of the "Shifted Ace lake sulfate" represents sulfate of non-equilibrium MSR at 5.5 m depth in Ace lake but the values are shifted by replacing Ace lake water with the average MaRB water; "EQ. sulfate" represents sulfate calculated by Equation (13) using the average water isotope data and at temperature 8.3 °C, i.e., the mean of Mean Annual Temperature (MAT) within Marsyangdi River Basin.

sequentially from the same $BaSO_4$ sample are nearly the same (Bao and Thiemens 2000), which suggests that O_2 yields between 10–30% will produce the same $\Delta'^{17}O$ but does not exclude the possibility that these O_2 with lower than 30% yield are systematically different from the 100% O_2 in the $\Delta'^{17}O$. Cowie and Johnston (2016) concluded from a regression line generated by 38 analyses of an inhouse $BaSO_4$ standard that the ~50%-yield processes have followed a slope of 0.5301 which is analytically unresolvable from the reference slope 0.5305 when calculating the $\Delta'^{17}O$. If 0.5301 were indeed the diagnostic θ value for the partial O_2 generation reaction, the $\Delta'^{17}O$ calculated using the raw $\delta^{18}O$ and $\delta^{17}O$ of the ~50%-yielded O_2 would represent the $\Delta'^{17}O$ of quantitative O_2 from $BaSO_4$. Unfortunately, the underlying reaction mechanism for the spread of the inhouse raw $\delta^{18}O$ and $\delta^{17}O$ data is not known *a priori.* Therefore the diagnostic θ value for the partial O_2 generation from $BaSO_4$ may not be close to the reference slope 0.5305. As mentioned in the riverine sulfate cases, this is one of the uncertainties that have prevented us from quantitatively interpreting the small sulfate $\Delta'^{17}O$ variations.

FUTURE OPPORTUNITIES

Small triple oxygen isotope variation in sulfate, measured by $\Delta'^{17}O_{SO_4}$, is a high-dimensional parameter that reveals the dynamics and pathway of sulfur cycling at present and in the past. The four sulfate endmembers we identified in this chapter are going to help us to interpret the measured small $\Delta'^{17}O_{SO_4}$. As discussed above, uncertainties exist even for these endmembers. There are ample research opportunities along this line, and here we outline the most pressing ones.

Calibrating small $\Delta'^{17}O_{SO_4}$ ***measurement.*** Accurate measurement of $\Delta'^{17}O_{SO_4}$ is necessary to power the small $\Delta'^{17}O_{SO4}$ research. Although uncertainty for $\Delta'^{17}O_{SO_4}$ measurement can reach 0.01‰ or less (Cowie and Johnston 2016), the O_2 generation reactions all have only partial O_2 yields. Such obtained $\Delta'^{17}O$ values are inherently less robust or stable than those of quantitative yield. Linking $\Delta'^{17}O_{SO_4}$ with that of water or O_2 at the intrinsic level demands a quantitative yield or well-calibrated θ values for partial-yield reactions. At this time, there is an urgent need to revisit the partial yield effect on triple oxygen isotope compositions of sulfate. Quantitative conversion of sulfate to carbon dioxide and equilibrating CO_2 and O_2 at high temperature assisted by a Pt catalyst (Mahata et al. 2013; Barkan et al. 2015) might be a way to resolve this problem, although this issue is not important when dealing with large ^{17}O anomalies.

Calibrating intrinsic triple oxygen isotope effects. Several EIEs, KIEs, and their associated θs determine sulfate triple oxygen isotope compositions. For now, only the equilibrium $^{18}\alpha_{SO_4-H_2O}$ is relatively converged in literature, while some of the other key parameters, e.g., $\alpha_{sulfite-H_2O}$ and $\alpha_{thiosulfate-H_2O}$, are exhibiting a range of values or entirely absent.

Calibrating reaction rate constants. Multiple electron transfers and thus multiple chemical reactions are involved in sulfur oxidation or sulfate reduction. Meanwhile, some intermediates exchange oxygen isotopes with water with different rate constants. These rates are competing with each other and determine the reversibility of a sulfur redox reaction and isotope equilibrium or non-equilibrium state of relevant intermediates. For some endmember cases, e.g. sulfite, its oxidation and oxygen exchange kinetics are well understood while others, e.g. oxidation and oxygen exchange kinetics for thiosulfate and tetrathionate, are poorly constrained or entirely unknown.

Sorting out reaction pathways. Sulfate can have different oxygen sources, and reaction pathways control the relative fractions of these different oxygen sources. Pyrite oxidation has the most geological implication. Molecular O_2 and water can both be incorporated into sulfate during pyrite oxidation. Several laboratory experiments have been conducted to constrain the relative proportions of O_2 and water in pyrite derived sulfate (Taylor et al. 1984a, Balci et al. 2007; Heidel et al. 2009; Tichomirowa and Junghans 2009; Heidel and Tichomirowa 2010; Kohl and Bao 2011). Nevertheless, factors controlling the reaction pathways and thus the relative fraction of incorporated O_2 in sulfate are still nebulous, and the observed results are not converging among different laboratories. Experiments using novel designs, e.g., ^{17}O label technique, are needed to understand reaction pathways, especially in pH-buffered solutions.

Knowing the role of microbes. Although biotic redox reaction is similar to the abiotic one to a great extent, it has unique characteristics. For example, the O_2 reduction and sulfur oxidation sites are often physically separated in enzymatic reactions (Kelly 1982; Balci et al. 2017); multiple sulfur oxidation pathways can occur concurrently in one microbe community (Bobadilla Fazzini et al. 2013); the reversibility of redox reactions is highly dependent on the energy status or thermodynamic potential (Wing and Halevy 2014). Well-controlled experiments and numerical models for abiotic redox reactions are essential to unsealing of the black boxes.

ACKNOWLEDGEMENTS

David Johnston and James Lyons are acknowledged for their constructive comments and suggestions. Xiao Tan provided editorial assistance. This study is financially supported by CAS "Light of West China" Program to XC and by the Strategic Priority Research Program (B) of Chinese Academy of Sciences (XDB18010104), Chinese Natural Science Foundation (41490635), and Jones Professorship to HB.

REFERENCES

Angert A, Rachmilevitch S, Barkan E, Luz B (2003) Effects of photorespiration, the cytochrome pathway, and the alternative pathway on the triple isotopic composition of atmospheric O_2. Global Biogeochem Cycles 17:1030

Angert A, Cappa CD, DePaolo DJ (2004) Kinetic ^{17}O effects in the hydrologic cycle: Indirect evidence and implications. Geochim Cosmochim Acta 68:3487–3495

Antler G, Turchyn AV, Rennie V, Herut B, Sivan O (2013) Coupled sulfur and oxygen isotope insight into bacterial sulfate reduction in the natural environment. Geochim Cosmochim Acta 118:98–117

Antler G, Turchyn AV, Ono S, Sivan O, Bosak T (2017) Combined ^{34}S, ^{33}S and ^{18}O isotope fractionations record different intracellular steps of microbial sulfate reduction. Geochim Cosmochim Acta 203:364–380

Balci N, Shanks WC, Mayer B, Mandernack KW (2007) Oxygen and sulfur isotope systematics of sulfate produced by bacterial and abiotic oxidation of pyrite. Geochim Cosmochim Acta 71:3796–3811

Balci N, Mayer B, Shanks WC, III, Mandernack KW (2012) Oxygen and sulfur isotope systematics of sulfate produced during abiotic and bacterial oxidation of sphalerite and elemental sulfur. Geochim Cosmochim Acta 77:335–351

Balci N, Brunner B, Turchyn AV (2017) Tetrathionate and elemental sulfur shape the isotope composition of sulfate in acid mine drainage. Front Microbiol 8:1564

Bao H (2015) Sulfate: A time capsule for Earth's O_2, O_3, and H_2O. Chem Geol 395:108–118

Bao HM (2006) Purifying barite for oxygen isotope measurement by dissolution and reprecipitation in a chelating solution. Anal Chem 78:304–309

Bao H (2019) Triple Oxygen Isotopes. Cambridge University Press, Cambridge

Bao HM, Thiemens MH (2000) Generation of O_2 from $BaSO_4$ using a CO_2-laser fluorination system for simultaneous analysis of $\delta^{18}O$ and $\delta^{17}O$. Anal Chem 72:4029–4032

Bao H, Campbell DA, Bockheim JG, Thiemens MH (2000a) Origins of sulphate in Antarctic dry-valley soils as deduced from anomalous ^{17}O compositions. Nature 407:499–502

Bao HM, Thiemens MH, Farquhar J, Campbell DA, Lee CCW, Heine K, Loope DB (2000b) Anomalous 17O compositions in massive sulphate deposits on the Earth. Nature 406:176–178

Bao H, Lyons JR, Zhou C (2008) Triple oxygen isotope evidence for elevated CO_2 levels after a Neoproterozoic glaciation. Nature 453:504–506

Bao H, Fairchild IJ, Wynn PM, Spoetl C (2009) Stretching the envelope of past surface environments: Neoproterozoic glacial lakes from Svalbard. Science 323:119–122

Bao H, Yu S, Tong DQ (2010) Massive volcanic SO_2 oxidation and sulphate aerosol deposition in Cenozoic North America. Nature 465:909–912

Bao H, Cao X, Hayles JA (2015) The confines of triple oxygen isotope exponents in elemental and complex mass-dependent processes. Geochim Cosmochim Acta 170:39–50

Bao H, Cao X, Hayles JA (2016) Triple oxygen isotopes: Fundamental relationships and applications. Annu Rev Earth Planet Sci 44:463–492

Barkan E, Luz B (2005) High precision measurements of $^{17}O/^{16}O$ and $^{18}O/^{16}O$ ratios in H_2O. Rapid Commun Mass Spectrom 19:3737–3742

Barkan E, Luz B (2007) Diffusivity fractionations of $H_2{}^{16}O/H_2{}^{17}O$ and $H_2{}^{16}O/H_2{}^{18}O$ in air and their implications for isotope hydrology. Rapid Commun Mass Spectrom 21:2999–3005

Barkan E, Luz B (2011) The relationships among the three stable isotopes of oxygen in air, seawater and marine photosynthesis. Rapid Commun Mass Spectrom 25:2367–2369

Barkan E, Musan I, Luz B (2015) High-precision measurements of delta O−17 and O−17(excess) of NBS19 and NBS18. Rapid Commun Mass Spectrom 29:2219–2224

Berner RA, Canfield DE (1989) A new model for atmospheric oxygen over Phanerozoic time. Am J Sci 289:333–361

Bertran E, Waldeck A, Wing BA, Halevy I, Leavitt WD, Bradley AS, Johnston DT (2020) Oxygen isotope effects during microbial sulfate reduction: Applications to sediment cell abundances. ISME J

Betts RH, Voss RH (1970) The kinetics of oxygen exchange between sulfite ion and water. Can J Chem 48:2035–2041

Betts RH, Libich S (1971) 18O transfer in system thiosulfate-sulfite–water: An example of a set of consecutive reversible first order rate processes. Can J Chem 49:180–186

Bigeleisen J, Wolfsberg M (1958) Theoretical and experimental aspects of isotope effects in chemical kinetics. *In*: Adv Chem Phys. John Wiley & Sons, Inc., p 15–76

Bindeman IN, Bayon G, Palandri J (2019) Triple oxygen isotope investigation of fine-grained sediments from major world's rivers: Insights into weathering processes and global fluxes into the hydrosphere. Earth Planet Sci Lett 528

Bobadilla Fazzini RA, Cortes MP, Padilla L, Maturana D, Budinich M, Maass A, Parada P (2013) Stoichiometric modeling of oxidation of reduced inorganic sulfur compounds (Riscs) in *Acidithiobacillus thiooxidans*. Biotechnol Bioeng 110:2242–2251

Borilova S, Mandl M, Zeman J, Kucera J, Pakostova E, Janiczek O, Tuovinen OH (2018) Can sulfate be the first dominant aqueous sulfur species formed in the oxidation of pyrite by *Acidithiobacillus ferrooxidans*? Front Microbiol 9:3134

Bottrell SH, Newton RJ (2006) Reconstruction of changes in global sulfur cycling from marine sulfate isotopes. Earth Sci Rev 75:59–83

Brunner B, Bernasconi SM, Kleikemper J, Schroth MH (2005) A model for oxygen and sulfur isotope fractionation in sulfate during bacterial sulfate reduction processes. Geochim Cosmochim Acta 69:4773–4785

Brunner B, Mielke RE, Coleman M (2006) Abiotic oxygen isotope equilibrium fractionation between sulfite and water, AGU Fall Meeting Abstracts, pp. V11C–0601

Brunner B, Yu J-Y, Mielke RE, MacAskill JA, Madzunkov S, McGenity TJ, Coleman M (2008) Different isotope and chemical patterns of pyrite oxidation related to lag and exponential growth phases of *Acidithiobacillus ferrooxidans* reveal a microbial growth strategy. Earth Planet Sci Lett 270:63–72

Brunner B, Einsiedl F, Arnold GL, Müller I, Templer S, Bernasconi SM (2012) The reversibility of dissimilatory sulphate reduction and the cell-internal multi-step reduction of sulphite to sulphide: Insights from the oxygen isotope composition of sulphate. Isotopes Environ Health Stud 48:33–54

Burton HR, Barker RJ (1979) Sulfur chemistry and microbiological fractionation of sulfur isotopes in a saline Antarctic lake. Geomicrobiol J 1:329–340

Caldeira CL, Ciminelli VST, Osseo-Asare K (2010) The role of carbonate ions in pyrite oxidation in aqueous systems. Geochim Cosmochim Acta 74:1777–1789

Calmels D, Gaillardet J, Brenot A, France-Lanord C (2007) Sustained sulfide oxidation by physical erosion processes in the Mackenzie River basin: Climatic perspectives. Geology 35:1003–1006

Cao X, Bao H (2017) Redefining the utility of the three-isotope method. Geochim Cosmochim Acta 212:16–32

Cao X, Bao H, Peng Y (2019) A kinetic model for isotopologue signatures of methane generated by biotic and abiotic CO_2 methanation. Geochim Cosmochim Acta 249:59–75

Cao X, Liu Y (2011) Equilibrium mass-dependent fractionation relationships for triple oxygen isotopes. Geochim Cosmochim Acta 75:7435–7445

Chandra AP, Gerson AR (2010) The mechanisms of pyrite oxidation and leaching: A fundamental perspective. Surf Sci Rep 65:293–315

Chiba H, Sakai H (1985) Oxygen isotope exchange rate between dissolved sulfate and water at hydrothermal temperatures. Geochim Cosmochim Acta 49:993–1000

Claypool GE, Holser WT, Kaplan IR, Sakai H, Zak I (1980) The age curves of sulfur and oxygen isotopes in marine sulfate and their mutual interpretation. Chem Geol 28:199–260

Cowie BR, Johnston DT (2016) High-precision measurement and standard calibration of triple oxygen isotopic compositions ($\delta^{18}O$, $\Delta'^{17}O$) of sulfate by F_2 laser fluorination. Chem Geol 440:50–59

Craig H (1961) Standard for reporting concentrations of deuterium and oxygen–18 in natural waters. Science 133:1833–1834

Crockford PW, Hayles JA, Bao H, Planavsky NJ, Bekker A, Fralick PW, Halverson GP, Thi Hao B, Peng Y, Wing BA (2018) Triple oxygen isotope evidence for limited mid-Proterozoic primary productivity. Nature 559:613–616

Crockford PW, Cowie BR, Johnston DT, Hoffman PF, Sugiyama I, Pellerin A, Bui TH, Hayles J, Halverson GP, Macdonald FA, Wing BA (2016) Triple oxygen and multiple sulfur isotope constraints on the evolution of the post-Marinoan sulfur cycle. Earth Planet Sci Lett 435:74–83

Crockford PW, Kunzmann M, Bekker A, Hayles J, Bao H, Halverson GP, Peng Y, Bui TH, Cox GM, Gibson TM, Wörndle S (2019) Claypool continued: Extending the isotopic record of sedimentary sulfate. Chem Geol 513:200–225

Dauphas N, Schauble EA (2016) Mass fractionation laws, mass-independent effects, and isotopic anomalies. Annu Rev Earth Planet Sci 44:709–783

Druschel GK, Hamers RJ, Banfield JF (2003) Kinetics and mechanism of polythionate oxidation to sulfate at low pH by O_2 and Fe^{3+}. Geochim Cosmochim Acta 67:4457–4469

Eldridge DL, Mysen BO, Cody GD (2018) Experimental estimation of the bisulfite isomer quotient as a function of temperature: Implications for sulfur isotope fractionations in aqueous sulfite solutions. Geochim Cosmochim Acta 220:309–328

Feng C, Tollin G, Enernark JH (2007) Sulfite oxidizing enzymes. Biochim Biophys Acta Proteins Proteom 1774:527–539

Friedrich CG, Rother D, Bardischewsky F, Quentmeier A, Fischer J (2001) Oxidation of reduced inorganic sulfur compounds by bacteria: Emergence of a common mechanism? Appl Environ Microbiol 67:2873–2882

Fritz P, Basharmal GM, Drimmie RJ, Ibsen J, Qureshi RM (1989) Oxygen isotope exchange between sulfate and water during bacterial reduction of sulfate. Chem Geol 79:99–105

Gázquez F, Morellón M, Bauska T, Herwartz D, Surma J, Moreno A, Staubwasser M, Valero-Garcés B, Delgado-Huertas A, Hodell DA (2018) Triple oxygen and hydrogen isotopes of gypsum hydration water for quantitative paleo-humidity reconstruction. Earth Planet Sci Lett 481:177–188

Geng L, Schauer AJ, Kunasek SA, Sofen ED, Erbland J, Savarino J, Allman DJ, Sletten RS, Alexander B (2013) Analysis of oxygen–17 excess of nitrate and sulfate at sub-micromole levels using the pyrolysis method. Rapid Commun Mass Spectrom 27:2411–2419

Ghosh W, Dam B (2009) Biochemistry and molecular biology of lithotrophic sulfur oxidation by taxonomically and ecologically diverse bacteria and archaea. FEMS Microbiol Rev 33:999–1043

Goldhaber MB (1983) Experimental study of metastable sulfur oxyanion formation during pyrite oxidation at pH 6–9 and 30 °C. Am J Sci 283:193–217

Griffith EM, Paytan A (2012) Barite in the ocean – occurrence, geochemistry and palaeoceanographic applications. Sedimentology 59:1817–1835
Guo W, Zhou C (2019) Triple oxygen isotope fractionation in the DIC-H_2O-CO_2 system: A numerical framework and its implications. Geochim Cosmochim Acta 246:541–564
Hanor JS (2000) Barite–celestine geochemistry and environments of formation. Rev Mineral Geochem 40:193–275
Harris E, Sinha B, Van Pinxteren D, Tilgner A, Fomba KW, Schneider J, Roth A, Gnauk T, Fahlbusch B, Mertes S, Lee T (2013) Enhanced role of transition metal ion catalysis during in-cloud oxidation of SO_2. Science 340:727–730
Hayles JA, Cao X, Bao H (2017) The statistical mechanical basis of the triple isotope fractionation relationship. Geochem Perspect Lett 3:1–11
Heidel C, Tichomirowa M (2010) The role of dissolved molecular oxygen in abiotic pyrite oxidation under acid pH conditions—Experiments with ^{18}O-enriched molecular oxygen. Appl Geochem 25:1664–1675
Heidel C, Tichomirowa M (2011) The isotopic composition of sulfate from anaerobic and low oxygen pyrite oxidation experiments with ferric iron—New insights into oxidation mechanisms. Chem Geol 281:305–316
Heidel C, Tichomirowa M, Junghans M (2009) The influence of pyrite grain size on the final oxygen isotope difference between sulphate and water in aerobic pyrite oxidation experiments. Isotopes Environ Health Stud 45:321–342
Hemingway JD, Olson H, Turchyn AV, Tipper ET, Bickle MJ, Johnston DT (2020) Triple oxygen isotope insight into terrestrial pyrite oxidation. Proc Natl Acad Sci USA 117:7650–7657
Hodgskiss MSW, Crockford PW, Peng Y, Wing BA, Horner TJ (2019) A productivity collapse to end Earth's Great Oxidation. Proc Natl Acad Sci USA 116:17207–17212
Holt BD, Kumar R, Cunningham PT (1981) Oxygen−18 study of the aqueous-phase oxidation of sulfur dioxide. Atmos Environ 15:557–566
Horner DA, Connick RE (2003) Kinetics of oxygen exchange between the two isomers of bisulfite ion, disulfite ion ($S_2O_5^{2-}$), and water as studied by oxygen−17 nuclear magnetic resonance spectroscopy. Inorg Chem 42:1884–1894
Hulston JR, Thode HG (1965) Variations in S33, S34, and S36 contents of meteorites and their relation to chemical and nuclear effects. J Geophys Res 70:3475–3484
Jørgensen BB (1977) Sulfur cycle of a coastal marine sediment (Limfjorden, Denmark). Limnol Oceanogr 22:814–832
Jørgensen BB (1982) Mineralization of organic matter in the sea bed—the role of sulphate reduction. Nature 296:643–645
Kasten S, Jørgensen BB (2000) Sulfate reduction in marine sediments. *In*: Marine Geochemistry. Schulz HD, Zabel M, (eds). Springer Berlin Heidelberg, Berlin, Heidelberg, p 263–281
Kelly DP (1982) Biochemistry of the chemolithotrophic oxidation of inorganic sulphur. Philos Trans R Soc Lond B Biol Sci 298:499–528
Kelly DP (2003) Microbial inorganic sulfur oxidation: The APS pathway. *In*: Biochemistry and Physiology of Anaerobic Bacteria. Ljungdahl LG, Adams MW, Barton LL, Ferry JG, Johnson MK, (eds). Springer New York, New York, NY, p 205–219
Killingsworth BA, Bao H, Kohl IE (2018) Assessing pyrite-derived sulfate in the Mississippi river with four years of sulfur and triple-oxygen isotope data. Environ Sci Technol 52:6126–6136
Klatt JM, Polerecky L (2015) Assessment of the stoichiometry and efficiency of CO^2 fixation coupled to reduced sulfur oxidation. Front Microbiol 6
Kohl I, Bao H (2011) Triple-oxygen-isotope determination of molecular oxygen incorporation in sulfate produced during abiotic pyrite oxidation (pH=2–11). Geochim Cosmochim Acta 75:1785–1798
Kroopnick P, Craig H (1972) Atmospheric oxygen: Isotopic composition and solubility fractionation. Science 175:54–55
Krouse HR, Gould WD, McCready RGL, Rajan S (1991) ^{18}O incorporation into sulphate during the bacterial oxidation of sulphide minerals and the potential for oxygen isotope exchange between O_2, H_2O and oxidized sulphur intermediates. Earth Planet Sci Lett 107:90–94
Kuo DTF, Kirk DW, Jia CQ (2006) The chemistry of aqueous S(IV)–Fe–O_2 system: state of the art. J Sulphur Chem 27:461–530
Lauro FM, DeMaere MZ, Yau S, Brown MV, Ng C, Wilkins D, Raftery MJ, Gibson JA, Andrews-Pfannkoch C, Lewis M, Hoffman JM (2011) An integrative study of a meromictic lake ecosystem in Antarctica. ISME J 5:879–895
Lente G, Fábián I (2002) Kinetics and mechanism of the oxidation of sulfur(IV) by iron(III) at metal ion excess. J Chem Soc, Dalton Trans:778–784
Li S, Levin NE, Chesson LA (2015) Continental scale variation in ^{17}O-excess of meteoric waters in the United States. Geochim Cosmochim Acta 164:110–126
Li B, Yeung LY, Hu H, Ash JL (2019) Kinetic and equilibrium fractionation of O_2 isotopologues during air-water gas transfer and implications for tracing oxygen cycling in the ocean. Mar Chem 210:61–71
Lloyd RM (1968) Oxygen isotope behavior in the Sulfate–water System. J Geophys Res 73:6099–6110
Lloyd RM (1967) Oxygen−18 composition of oceanic sulfate. Science 156:1228–1231
Luther GW (1987) Pyrite oxidation and reduction: Molecular orbital theory considerations. Geochim Cosmochim Acta 51:3193–3199
Luz B, Barkan E (2010) Variations of $^{17}O/^{16}O$ and $^{18}O/^{16}O$ in meteoric waters. Geochim Cosmochim Acta 74:6276–6286

Mahata S, Bhattacharya SK, Wang C-H, Liang M-C (2013) Oxygen isotope exchange between O_2 and CO_2 over hot platinum: an innovative technique for measuring $\Delta^{17}O$ in CO_2. Anal Chem 85:6894–6901
Mazumdar A, Goldberg T, Strauss H (2008) Abiotic oxidation of pyrite by Fe(III) in acidic media and its implications for sulfur isotope measurements of lattice-bound sulfate in sediments. Chem Geol 253:30–37
McCrea JM (1950) On the isotopic chemistry of carbonates and a paleotemperature scale. J Chem Phys 18:849–857
McCready RGL, Krouse HR (1982) Sulfur isotope fractionation during the oxidation of elemental sulfur by *Thiobacilli* in a Solonetzic soil. Can J Soil Sci 62:105–110
McKinney CR, McCrea JM, Epstein S, Allen HA, Urey HC (1950) Improvements in mass spectrometers for the measurement of small differences in isotope abundance ratios. Rev Sci Instrum 21:724–730
Miller MF (2002) Isotopic fractionation and the quantification of ^{17}O anomalies in the oxygen three-isotope system: an appraisal and geochemical significance. Geochim Cosmochim Acta 66:1881–1889
Mizutani Y, Rafter TA (1973) Isotopic behaviour of sulphate oxygen in the bacterial reduction of sulphate. Geochem J 6:183–191
Mook WG (2000) Environmental isotopes in the hydrological cycle: Principles and applications, Vol. I: Introduction —Theory, Methods, Review. *In*: Isotope Effects. UNESCO/IAEA, Paris,
Moses CO, Herman JS (1991) Pyrite oxidation at circumneutral pH. Geochim Cosmochim Acta 55:471–482
Moses CO, Kirk Nordstrom D, Herman JS, Mills AL (1987) Aqueous pyrite oxidation by dissolved oxygen and by ferric iron. Geochim Cosmochim Acta 51:1561–1571
Müller IA, Brunner B, Coleman M (2013a) Isotopic evidence of the pivotal role of sulfite oxidation in shaping the oxygen isotope signature of sulfate. Chem Geol 354:186–202
Müller IA, Brunner B, Breuer C, Coleman M, Bach W (2013b) The oxygen isotope equilibrium fractionation between sulfite species and water. Geochim Cosmochim Acta 120:562–581
Nriagu JO (1972) Stability of vivianite and ion-pair formation in the system $Fe_3(PO_4)_2$–H_3PO_4–H_2O. Geochim Cosmochim Acta 36:459–470
Oba Y, Poulson SR (2009) Oxygen isotope fractionation of dissolved oxygen during abiological reduction by aqueous sulfide. Chem Geol 268:226–232
Pack A, Herwartz D (2014) The triple oxygen isotope composition of the Earth mantle and understanding variations in terrestrial rocks and minerals. Earth Planet Sci Lett 390:138–145
Passey BH, Ji H (2019) Triple oxygen isotope signatures of evaporation in lake waters and carbonates: A case study from the western United States. Earth Planet Sci Lett 518:1–12
Peng Y, Bao H, Zhou C, Yuan X (2011) ^{17}O-depleted barite from two Marinoan cap dolostone sections, South China. Earth Planet Sci Lett 305:21–31
Pryor WA, Tonellat U (1967) Nucleophilic displacements at sulfur. III. The exchange of oxygen−18 between sodium thiosulfate−^{18}O and water. J Am Chem Soc 89:3379–3386
Rennie VCF, Turchyn AV (2014) Controls on the abiotic exchange between aqueous sulfate and water under laboratory conditions. Limnol Oceanogr Methods 12:166–173
Reuer MK, Barnett BA, Bender ML, Falkowski PG, Hendricks MB (2007) New estimates of Southern Ocean biological production rates from O_2/Ar ratios and the triple isotope composition of O_2. Deep Sea Res Part I Oceanogr Res Pap 54:951–974
Rimstidt JD, Vaughan DJ (2003) Pyrite oxidation: A state-of-the-art assessment of the reaction mechanism. Geochim Cosmochim Acta 67:873–880
Roberts D, Roberts JL, Gibson JAE, McMinn A, Heijnis H (1999) Palaeohydrological modelling of Ace Lake, Vestfold Hills, Antarctica. Holocene 9:515–520
Rosso KM, Vaughan DJ (2006) Reactivity of sulfide mineral surfaces. Rev Mineral Geochem 61:557–607
Sand W, Gerke T, Hallmann R, Schippers A (1995) Sulfur chemistry, biofilm, and the (in)direct attack mechanism - a critical-evaluation of bacterial leaching. Appl Microbiol Biotechnol 43:961–966
Savarino J, Lee CCW, Thiemens MH (2000) Laboratory oxygen isotopic study of sulfur (IV) oxidation: Origin of the mass-independent oxygen isotopic anomaly in atmospheric sulfates and sulfate mineral deposits on Earth. J Geophys Res Atmos 105:29079–29088
Savarino J, Alexander B, Darmohusodo V, Thiemens MH (2001) Sulfur and oxygen isotope analysis of sulfate at micromole levels using a pyrolysis technique in a continuous flow system. Anal Chem 73:4457–4462
Schauble EA, Young ED (2021) Mass dependence of equilibrium oxygen isotope fractionation in carbonate, nitrate, oxide, perchlorate, phosphate, silicate, and sulfate minerals. Rev Mineral Geochem 86:137–178
Schauer AJ, Kunasek SA, Sofen ED, Erbland J, Savarino J, Johnson BW, Amos HM, Shaheen R, Abaunza M, Jackson TL, Thiemens MH (2012) Oxygen isotope exchange with quartz during pyrolysis of silver sulfate and silver nitrate. Rapid Commun Mass Spectrom 26:2151–2157
Schippers A, Jozsa PG, Sand W (1996) Sulfur chemistry in bacterial leaching of pyrite. Appl Environ Microbiol 62:3424–3431
Sharp ZD, Wostbrock JAG, Pack A (2018) Mass-dependent triple oxygen isotope variations in terrestrial materials. Geochem Perspect Lett 7:27–31
Singer PC (1972) Anaerobic control of phosphate by ferrous iron. J Water Pollut Control Fed 44:663–669

Singer PC, Stumm W (1970) Acidic mine drainage: The rate-determining step. Science 167:1121–1123
Smith LA, Hendry MJ, Wassenaar LI, Lawrence J (2012) Rates of microbial elemental sulfur oxidation and ^{18}O and ^{34}S isotopic fractionation under varied nutrient and temperature regimes. Appl Geochem 27:186–196
Spencer RJ (2000) Sulfate minerals in evaporite deposits. Rev Mineral Geochem 40:173–192
Stefánsson A (2007) Iron(III) hydrolysis and solubility at 25 °C. Environ Sci Technol 41:6117–6123
Sun T, Socki RA, Bish DL, Harvey RP, Bao H, Niles PB, Cavicchioli R, Tonui E (2015) Lost cold Antarctic deserts inferred from unusual sulfate formation and isotope signatures. Nat Commun 6:7579
Surma J, Assonov S, Bolourchi MJ, Staubwasser M (2015) Triple oxygen isotope signatures in evaporated water bodies from the Sistan Oasis, Iran. Geophys Res Lett 42:8456–8462
Taylor BE, Wheeler MC, Nordstrom DK (1984a) Stable isotope geochemistry of acid mine drainage: Experimental oxidation of pyrite. Geochim Cosmochim Acta 48:2669–2678
Taylor BE, Wheeler MC, Nordstrom DK (1984b) Isotope composition of sulphate in acid mine drainage as measure of bacterial oxidation. Nature 308:538–541
Thiemens MH (2006) History and applications of mass-independent isotope effects. Annu Rev Earth Planet Sci 34:217–262
Thurston RS, Mandernack KW, Shanks WC, III (2010) Laboratory chalcopyrite oxidation by *Acidithiobacillus ferrooxidans*: Oxygen and sulfur isotope fractionation. Chem Geol 269:252–261
Tichomirowa M, Junghans M (2009) Oxygen isotope evidence for sorption of molecular oxygen to pyrite surface sites and incorporation into sulfate in oxidation experiments. Appl Geochem 24:2072–2092
Turchyn AV, Brüchert V, Lyons TW, Engel GS, Balci N, Schrag DP, Brunner B (2010) Kinetic oxygen isotope effects during dissimilatory sulfate reduction: A combined theoretical and experimental approach. Geochim Cosmochim Acta 74:2011–2024
Van Stempvoort DR, Krouse HR (1993) Controls of $\delta^{18}O$ in sulfate: Review of experimental data and application to specific environments. *In*: Environmental Geochemistry of Sulfide Oxidation. Vol 550. American Chemical Society, p 446–480
Vera M, Schippers A, Sand W (2013) Progress in bioleaching: Fundamentals and mechanisms of bacterial metal sulfide oxidation-part A. Appl Microbiol Biotechnol 97:7529–7541
Waldeck AR, Cowie BR, Bertran E, Wing BA, Halevy I, Johnston DT (2019) Deciphering the atmospheric signal in marine sulfate oxygen isotope composition. Earth Planet Sci Lett 522:12–19
Wankel SD, Bradley AS, Eldridge DL, Johnston DT (2014) Determination and application of the equilibrium oxygen isotope effect between water and sulfite. Geochim Cosmochim Acta 125:694–711
Wing BA, Halevy I (2014) Intracellular metabolite levels shape sulfur isotope fractionation during microbial sulfate respiration. PNAS 111:18116–18125
Wortmann UG, Chernyavsky B, Bernasconi SM, Brunner B, Böttcher ME, Swart PK (2007) Oxygen isotope biogeochemistry of pore water sulfate in the deep biosphere: Dominance of isotope exchange reactions with ambient water during microbial sulfate reduction (ODP Site 1130). Geochim Cosmochim Acta 71:4221–4232
Xu Y, Schoonen MAA (1995) The stability of thiosulfate in the presence of pyrite in low-temperature aqueous solutions. Geochim Cosmochim Acta 59:4605–4622
Young ED, Galy A, Nagahara H (2002) Kinetic and equilibrium mass-dependent isotope fractionation laws in nature and their geochemical and cosmochemical significance. Geochim Cosmochim Acta 66:1095–1104
Zak I, Sakai H, Kaplan IR (1980) Factors controlling $^{18}O/^{16}O$ and $^{34}S/^{32}S$ isotope rations of ocean sulfates, evaporites, and interstitial sulfates from modern deep sea sediments. *In*: Isotope marine chemistry. Goldberg ED, Horibe Y, Sakurashi K, (eds). Rokakuho, Tokyo, p 339–373
Zeebe RE (2010) A new value for the stable oxygen isotope fractionation between dissolved sulfate ion and water. Geochim Cosmochim Acta 74:818–828
Zhang JZ, Millero FJ (1991) The rate of sulfite oxidation in seawater. Geochim Cosmochim Acta 55:677–685
Ziegler K, Coleman ML, Mielke RE, Young ED (2010) Sources and contributions of oxygen during microbial pyrite oxidation: The triple oxygen isotopes of sulfate as a biosignature. Lunar and Planetary Science Conference, p. 2245